A Do-It-Yourself Small Footprint Potentiostat for Electrochemical Measurements

برقی کیمیائی تجربات کے لیے مختصر ہیئت کا برقی کیمیائی صلاحیت پیما

Rimsha Touqir

Acknowledgements

First and foremost, all praise and thanks are for Allah, whose blessings, guidance, and mercy enabled me to reach this stage. Without His support, none of this would have been possible.

I feel profoundly privileged and deeply grateful to my supervisor, Dr. Sabieh Anwar, whose mentorship has been the cornerstone of this entire thesis. His guidance nurtured my understanding of electronics from the very basics to a level I could never have imagined at the start. His patience, wisdom, and unwavering support not only shaped me as a researcher but also inspired me to think critically, explore fearlessly, and grow as a learner. I am truly honored to have had the opportunity to learn under his supervision and guidance, and I will always remain grateful for the remarkable journey of knowledge and growth he provided.

I am sincerely thankful to Jamal, who actively collaborated with me on this project. His professionalism, insights, and support in executing experiments and analyzing results greatly contributed to the successful completion of this work.

I would also like to sincerely thank Sir Nouman and Sir Salman for their guidance and support, which helped me pursue research effectively and discover my interest in electronics.

My deepest appreciation goes to the Physlab team for providing the space, equipment, and environment that made this thesis possible. Their support and welcoming atmosphere played a crucial role in the progress of my research.

I would also like to express my heartfelt gratitude to my mother and siblings for their constant encouragement, prayers, and emotional support throughout this journey. Their belief in me kept me strong at every step.

Finally, I extend my thanks to everyone who supported me in any way, directly or indirectly, during the completion of this thesis.

موضوعِ مقالہ، حجتِ تحقیق

یہ تحقیقی مقالہ ایک کم لاگت، مائیکرو کنٹرولر پر مبنی خود ساختہ برقی کیمیائی صلاحیت پیما[a] کے ڈیزائن اور تیاری پر مبنی ہے، جس کا مقصد طلبہ، اساتذہ اور محققین کے لیے برقی کیمیائی[b] آلات تک آسان رسائی فراہم کرنا ہے۔ سائنسی ترقی کے باوجود، بیشتر سائنسی آلات اب بھی مہنگے اور عام اداروں یا شوقیہ سیکھنے والوں کی پہنچ سے باہر ہیں۔ یہی خلا اس بات کو اجاگر کرتا ہے کہ کم لاگت اور اوپن سورس آلات کی تیاری آج بھی سائنسی تعلیم و تحقیق کی ایک بنیادی ضرورت ہے تاکہ تحقیق اور تعلیم دونوں میں مساوی مواقع سب کو میسر ہوں۔

تیار کردہ برقی کیمیائی صلاحیت پیما DUE Arduino مائیکرو کنٹرولر اور عام دستیاب الیکٹرانک اجزاء پر مبنی ہے، جو صارفین کو یہ صلاحیت دیتا ہے کہ وہ کم لاگت میں اس آلے کو خود تیار کر کے برقی کیمیائی پیمائش کے اصولوں کو سمجھ اور اپنی ضرورت کے مطابق ترتیب دے سکیں۔ یہ آلہ دورانی وولٹیمیٹری[c] کی صلاحیت رکھتا ہے، جس کے کوائف[d] محقق اپنی مرضی کے مطابق متعین کر سکتے ہیں، تاکہ مختلف برقی کیمیائی خلیوں[e] میں لچکدار تجربات کیے جا سکیں۔

ہارڈ ویئر اور سافٹ ویئر کے تفصیلی تجزیے سے ظاہر ہوتا ہے کہ تیار کردہ نظام قابلِ اعتماد، درست اور لچکدار ہے، جو اسے تعلیمی، تحقیقی اور تجرباتی استعمال کے لیے بے حد موزوں بناتا ہے۔ اس مربوط امتزاج میں درست وولٹیج کنٹرول، حساس کرنٹ پیمائش، اور حقیقی وقت میں ڈیٹا کے حصول کی صلاحیت شامل ہے۔ یہ خود کار نظام اس طرح ڈیزائن کیا گیا ہے کہ کم لاگت کے باوجود مستحکم کارکردگی، برقی شور میں کم سے کم مداخلت، اور وسیع تعددی[f] ردِ عمل فراہم کرے۔ DUE Arduino کی تیز رفتار سیمپلنگ اور سافٹ ویئر ترتیب نہ صرف برقی کیمیائی عمل کی باریک تبدیلیوں کو درستگی سے ناپتی ہے بلکہ برقی کیمیائی عمل کے دوران وولٹیج میں بتدریج تبدیلی کے نتیجے میں پیدا ہونے والے برقی رویہ کے ردِ عمل کو نہایت ہمواری سے ظاہر کرتی ہے، جس سے آئناتی ذرات کی حرکت اور ان کے تبادلے کے عمل کا درست مشاہدہ ممکن ہوتا ہے۔ یہ خصوصیات اِس آلے کو تحقیقی اور تدریسی مقاصد کے لیے ایک مؤثر اور قابلِ اعتماد آلہ بناتی ہیں۔ اس کا تہ بہ تہ[g] ڈیزائن شوقیہ سیکھنے والوں کو اپنی ضروریات کے مطابق نظام میں ترمیم اور توسیع کی سہولت فراہم کرتا ہے۔

a Potentiostat

b Electrochemical

c Cyclic Voltammetry

d Parameters

e Electrochemical Cell

f Wide range

g Modular

Abstract

This work presents a low cost, microcontroller based electrochemical potentiostat that is intended for educational purposes and small experimental applications. The device allows access to electrochemical measurement capabilities for students, hobbyist researchers, and small laboratories without dependence on expensive commercial instrumentation. This provides a simple and inexpensive setup that allows the practical exploration of electrochemical principles in situations where regular instruments are not available.

The potentiostat is built around an Arduino DUE with commonly available electronic components. It provides the facility of cyclic voltammetry with parameters that can be varied and allows conducting experiments with a wide range of electrochemical cells. This modular architecture allows users to modify and extend the system according to experimental needs, thus helping hands-on learning and exploring various reactions.

Tests of both hardware and software indicate that the system works reliably and provides results sufficiently accurate for educational or experimental purposes. The developed apparatus provided stable voltage control, sensitive current measurement, and real-time data acquisition with low electrical noise. High speed sampling and user configurable software enable the detection of subtle changes in voltage and current, reflecting dynamic ionic movement and related electrochemical processes.

The work underlines the possibility that low-cost, self assembled instrumentation can help bridge theoretical teaching and hands-on experimentation. The device makes electrochemical measurements more accessible, thereby supporting education and preliminary research, building up knowledge, experimentation, and skills in electronics and electrochemistry.

Contents

List of Figures

List of Tables

Chapter 1

Introduction

Electrochemistry belongs to the core of physical science that explores the interrelation between electrical energy and chemical change, having applications in energy storage, environmental monitoring and biological [1]. In order to translate theoretical electrochemical principle into measurable parameters, we need some tools to understand and investigate redox process, electrode kinetics and reaction mechanism. Building upon the foundation of electrochemistry, the device called the potentiostat its serves as a basic analytical tool that facilitates the experimental study of electrochemical reactions by precisely controlling and recording electrode potential and current [2]. However, the elevated expense and intricacy of commercial potentiostats presents a considerable obstacle to their widespread utilization, especially in educational and small-scale research settings with limited budget [3].

This thesis addresses the necessity for an accessible and cost-effective alternative

by introducing the construction of a D.I.Y. (Do-It-Yourself) microcontroller-based potentiostat. The suggested architecture provides a cost-effective and flexible solution utilizing readily accessible components, including the Arduino DUE and operational amplifiers. It enables precise cyclic voltammetry measurements that renders it suitable for educational purposes, hobbyist experimentation, and introductory research. Our initiatives at PhysLab seek to democratize electrochemical instrumentation by emphasizing open-source hardware and software. This study illustrates that low-cost platforms can achieve significant performance through meticulous system design, performance assessment, and comparison analysis with commercial systems.

1.1 Background

In recent years, the emergence of open-source electronics, notably the micro-controller based instrumentation platform has facilitated the development of cost-effective, customizable, and portable alternatives to conventional electrochemical systems. Recent advances in embedded electronics, open-source hardware platforms such as the Arduino, and accessible circuit simulation tools have collectively democratized the field of electrochemical measurements [3]. These developments have encouraged researchers and educators to design D.I.Y. potentiostats, offering an affordable entry point for electrochemical experimentation, academic training, and rapid prototyping. As worldwide focus intensifies on renewable energy and environmental sustainability, the demand for electrochemical technology and proficient practitioners is steadily rising so the need of D.I.Y. potentiostat projects have become increasingly popular for

enhancing access to electrochemical instruments, fostering creativity, and boosting experiential learning in STEM education. This project enhances existing initiatives by creating an affordable, Arduino-based potentiostat that facilitates fundamental electrochemical procedures while ensuring accessibility and adaptability for various users.

1.2 Objective

The primary objective of this thesis is to illustrate how multi-disciplinary design can yield powerful yet inexpensive research tools. The work presented in this thesis draws inspiration and contribution [5] from the growing movement that is to make science instrumentation more accessible, adaptable, and transparent, empowering researchers and students alike to explore the fundamentals of science using self-built and open-source systems.

To bridge science and accessibility, the principle aim is the design and developement of D.I.Y microcontroller based potentiostat. Thus it represents a significant step toward simplifying and modernizing electrochemical instrumentation. By integrating analog front-end circuitry with digital control and data acquisition systems, such a device can perform essential electrochemical function, controlling electrode potentials, measuring current responses, and communicating with a host computer for visualization and analysis.

A primary purpose is to guarantee compatibility with commercially avaliable potentiostat such as Gamry's potentiostat which was avaliable in our laboratory.

The device must be capable of executing cyclic voltammetry, a fundamental and commonly utilized approach in electrochemical analysis. The design will also accommodate the possibility of future expansion into additional techniques such as chronoamperometry, square-wave voltammetry, and linear sweep voltammetry.

In summary, the thesis seeks to develop a modular and open-source potentiostat with fully documented hardware and software, enabling users to easily modify, expand and integrate the system for new appplication thus fostering open innovation and collaboration in scientific instrumentation.

1.3 Scope Of Study

This project is explicitly defined to concentrate on the development, testing, and benchmarking of a single-channel potentiostat prototype. This delineated scope guarantees a focused and attainable result within the project's limitations.

The electrochemical emphasis is on cyclic voltammetry (CV). This technique entails linearly varying the potential squarely over time while recording the resultant current. CV is exceptionally appropriate for our study because of its pedagogical importance in imparting fundamental electrochemical principles and its effectiveness in assessing redox-active substances.

Two primary methods to hardware design configurations are examined. The breadboard prototype highlights adaptability and ease of alteration, rendering it suitable for educational and experimental environments. Second, the printed circuit

board (PCB) architecture provides a more durable, noise-resistant, and permanent solution for the gadget. It additionally facilitates the incorporation of interchangeable shields designed for certain applications.

The system's performance evaluation and validation are accomplished using several methodologies. This encompasses theoretical analysis of electrochemical behavior, direct comparison with commercial potentiostats regarding accuracy, noise levels, and response time, as well as the assessment of critical performance metrics including signal-to-noise ratio, dynamic range, resolution, scan rate stability, and reproducibility of voltammograms.

The created codebase facilitates real-time data gathering over serial transmission for program integration and customisation. Our potentiostat is constructed to be modular, facilitating the modification of essential experimental parameters. The software is also compatible with external tools for data visualization and logging thus improving usability.

Finally, limitations and restraints within our design are duly recognized. The device possesses numerous vital functions; nonetheless, it is constrained by limitations, including the utilization of an 12-bit DAC, dependence on Arduino Pulse Width Modulation for analog signal production, and restricted scan rate resolution. These constraints are acknowledged as opportunities for future improvement, refinement and there also remain the scope of upgradation by adding other electrochemical techniques too.

1.4 Significance

A significant contribution of this role lies in the realm of democratization of scientific instruments. This approach substantially reduces the cost of a relatively pricey instrument, thereby rendering electrochemical analysis accessible to students and researchers in institutions unable to afford commercial potentiostats. This effect is particularly pronounced in resource-constrained settings, including public schools, community colleges, and universities in the global south.

The project also facilitates the improvement of experiential learning in STEM. The device facilitates instructors in performing practical experiments, thereby bridging the divide between theory and application. This promotes active learning, critical thinking, and early involvement with scientific research methodologies and skills vital for a robust foundation in STEM education.

Furthermore, the project provides substantial assistance to the D.I.Y. and maker movements. This work promotes independent problem solving, engineering skill development, and creative tinkering by embracing open-source platforms such as Arduino and encouraging a do it yourself attitude. These attributes are essential for educating the forthcoming generation of scientists and engineers.

The primary aim of the project is to contribute to open-source scientific instruments. All design files, encompassing circuit schematics and source code, are designated for open sharing.

In addition to its educational applications, the low-cost potentiostat could be

utilized for environmental monitoring, biochemical sensing, and portable diagnostics. It lays the groundwork for future developments, including wireless communication, enhanced-resolution DACs, and multi-channel topologies, thus fostering continuous innovation in applied electrochemistry.

Chapter 2

Literature Review

Electrochemical instrumentation plays a vital role in modern analytical science. Techniques such as cyclic voltammetry, chronoamperometry, and electrochemical impedance spectroscopy are routinely employed in chemistry, biology, materials science, and environmental monitoring [6]. Central to these techniques is the potentiostat, a device that controls the voltage between electrodes in an electrochemical cell and measures the resulting current. This chapter explores the fundamental principles of electrochemical methods, examines some of the limitations of commercial potentiostats, reviews relevant open-source and microcontroller-based systems, and finally identifies key research gaps that this thesis aim to address.

2.1 Fundamentals of Electrochemical Methods

The basic principles of electrochemistry provide a solid foundation for the analytical characterization of chemical systems by studying the interaction between electrical factors (like potential, current, and charge) and chemical processes [7]. The Electrochemical techniques offer significant advantages in terms of sensitivity, detection limits and ability to study reactions thermo dynamically and kinetically by controlling and measuring redox processes at the electrolyte/electrode interface. The main techniques within this area can be divided based on the particular applied electrical signal to the system and the measured response, these procedures are useful for our work and are discussed below.

2.1.1 Cyclic voltammetry (CV)

Cyclic voltammetry is a direct current (DC) electrochemical technique, which records the response in a current while a potential scan is applied to the working electrode at a constant scan rate in the forward and reverse directions (Figure 2.1), once or several times [8]. Given its versatility and fundamental importance, this thesis is based on cyclic voltammetry. The term 'cyclic' in cyclic voltammetry means the repeated application of the potential scan and continuous current measurement. A detailed study of its principles, implementation, and applications will be presented in the upcoming chapters.

2.1.2 Amperometry

Amperometry [9] is an electroanalytical technique that involves the application of a constant reducing or oxidizing potential to a working electrode and the subsequent measurement of the resulting steady-state current as represented in Figure 2.1 .The main difference is that amperometry measures a constant current at a fixed potential to determine the analyte concentration, while cyclic voltammetry measures the current as a function of a continuously varying potential to study reaction reversibility and kinetics.

2.1.3 Chronoamperomtery (CA)

Chronoamperomtery (CA) is a potential step method (Figure 2.1) and is also known as constant potential bulk electrolysis, controlled potential amperometry, and potential pulse electrolysis. The simplest case, CA is the measurement of current vs. time due to a change (step, pulse) in potential [10]. Initially, the potential of the working electrode is held at such a value where no redox reaction (X) or no faradaic electron transfer are occuring, when the experiment starts we step the potential to a point that is sufficiently high to induce oxidation reaction or low to start a reduction reaction. In Fig(X), it can be observed that there is spike of current followed by the current decay. Breiefly describing the current spike is result of electrical double layer charging (non-Faradaic response) and the oxidation of electrolyte (Faradaic response). As the current is associated with the electrochemical species being oxidised, its concentration will gradually decrease with time which means the current will decay.

2.1.4 Chronopotentiometry (CP)

Chronopotentiometry (CP) is a galvanostatic method in which the current at the working electrode is held at a constant level for a given period of time and the working electrode potential and current are recorded as a function of time as shown in Figure 2.1. Typically, current is held constant between working and counter electrodes while potential is measured at the working electrode relative to the reference electrode. Researchers employ this method to study chemical reaction mechanisms and kinetics. It is also frequently used to study batteries and electrodeposition [11].

2.1.5 Electrochemical Impedance Spectroscopy

The technique of electrochemical impedance spectroscopy (Figure 2.1) is based on the perturbation of an electrochemical system in equilibrium or in steady state, via the application of a sinusoidal signal (ac voltage or ac current) over a wide range of frequencies and the monitoring of the sinusoidal response (current or voltage, respectively) of the system toward the applied perturbation [12]. This method has broad applications across fields such as corrosion analysis, semiconductor research, energy conversion and storage technologies, chemical sensing, biosensing, and even noninvasive diagnostic methods.

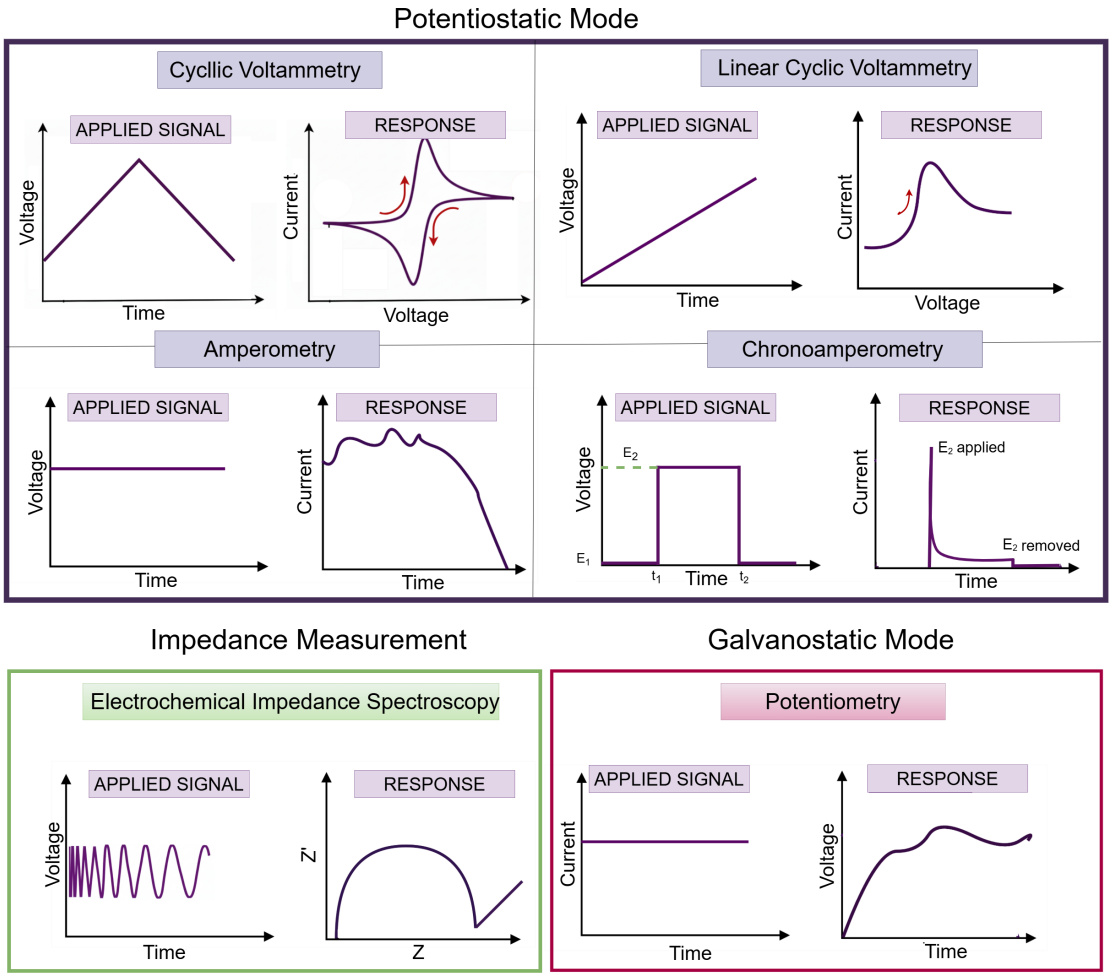

Figure 2.1: *Main Electrochemical techniques and, their input and output signals.*

2.2 Commercial Potentiostats: Features and Limitations

High-end commercial potentiostats, such as those manufactured by Gamry Instruments [13], CH Instruments [14], Osilla [15] and Metrohm Autolab [16] offer superior performance with high precision, low noise, and support for a wide range of techniques. These instruments typically includes high-resolution DACs (16-bit or higher), fast sampling ADCs, powerful onboard processors and advanced software for automation and data visualization. A potntiostat made by Gamry is very popular, and one such model is shown in Figure 2.2.

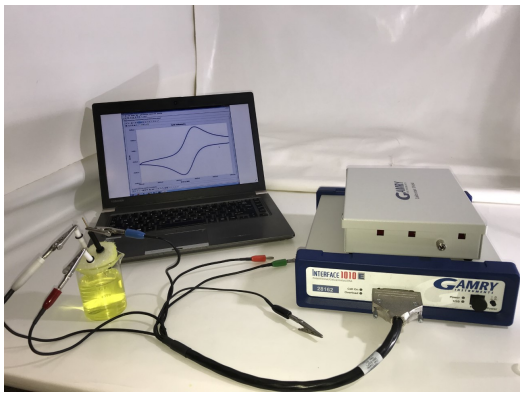

Figure 2.2: *Gamry Potentiostat setup in PhysLAB.*

However, these devices are often expensive as prices are mentioned in table2.1, and are therefore out of reach for many educational institutions, especially in developing regions. Furthermore, they are proprietary in both hardware and software, which limits their customizability for specific educational or research purposes.

Brand	Approximate Price Range (USD)	Model Specification
Ossila	\$1,000 – \$2,000	Entry-level potentiostats
Gamry Instruments	\$8,000 – \$15,000	Research-grade systems
CH Instruments (CHI)	\$5,000 – \$15,000	Mid-range research potentiostats
Metrohm / Autolab	\$7,000 – \$20,000	High-precision modular systems

Table 2.1: *Commercial potentiostat brands and approximate price ranges.*

2.3 Open-Source and D.I.Y. Potentiostats

In response to the elevated costs and limited adaptability of commercial potentiostat devices, the scientific and maker communities have created various open-source potentiostat alteratives. These devices are generally intended for educational purposes, fundamental research, or deployment in resource-limited settings, providing a cost-effective and versatile alternative to proprietary systems.

One initiative is CheapStat [17], created by Kevin J. O'Dell and colleagues. It is one of the early open-source potentiostats, constructed with inexpensive components. It is capable of executing fundamental procedures, including cyclic voltammetry (CV) and chronoamperometry. Nonetheless, its 8-bit resolution and restricted current range render it inadequate for more sophisticated applications necessitating greater precision and sensitivity.

Another noteworthy example is DStat [19], a more sophisticated open-source potentiostat that integrates a 16-bit DAC to enhance resolution and accuracy. DStat is appropriate for both educational purposes and small-scale research, rendering it an excellent option for budget-constrained academic laboratories.

The uWED [21] project embodies a concise and unique methodology, integrating microfluidic electrochemical measuring functionalities within a minimal spatial configuration. It is primarily intended for diagnostic and point-of-care applications, providing adequate performance in a portable format.

Although these open-source devices provide significant advantages for affordable and configurable applications, they also encounter various constraints. This encompasses reduced scan rates attributable to microcontroller processing limitations, diminished analog resolution, insufficient documentation that may limit precise reproduction, and constrained expandability that restricts adaption for sophisticated or evolving research requirements.

2.4 Micro-Controller based Instrumentation

Microcontrollers like the Arduino Uno, ESP32, and STM32 have been instrumental in facilitating the creation of affordable scientific instrumentation. These platforms provide fundamental characteristics such as digital control, PWM-based digital-to-analogue capabilities, and serial communication interfaces. Their extensive application in D.I.Y. electronics and STEM education is propelled by their cost-effectiveness, versatility, and the backing of a large user community.

In the realm of potentiostat development, microcontrollers can be configured to execute many essential functions. They may produce voltage ramps via pulse-width modulation (PWM) in conjunction with low-pass filtering, acquire current signals through onboard ADCs or external instrumentation amplifiers, and relay data to a

computer via USB or wireless communication modules.

Although these microcontroller-based devices typically do not possess the precision and reliability of premium commercial equipment, their utilization is on the rise across many environments. This include instructional laboratories, where economical tools are vital for experiential learning; portable field equipment, where compactness and cost-effectiveness are paramount; and budget-conscious research settings that necessitate swift and adaptable prototyping capabilities.

2.5 Research Gaps and Motivation

Notwithstanding the increasing prevalence of D.I.Y. and open-source potentiostat initiatives, certain constraints persist that hinder their wider use in both academic and practical research environments. Numerous current designs, including CheapStat, uMED, and DStat, despite their innovation, frequently exhibit two extremes—being either excessively simplistic for rigorous academic or analytical chemistry applications or overly sophisticated for secondary school or introductory undergraduate laboratories. For example, CheapStat employs an 8-bit DAC, providing 256 discrete voltage levels, so constraining resolution and rendering it inadequate for sensitive measurements where precision is paramount.

A significant disadvantage is the absence of thorough and accessible documentation, hindering replication and community-led enhancement. Moreover, modularity and scalability are frequently neglected in these initiatives. Most current systems are rigidly configured for a singular function, complicating the integration of new

methodologies such as differential pulse voltammetry or square wave voltammetry without necessitating a complete circuit redesign. While PWM-based analog signal creation is straightforward, it generates ripple and noise, particularly at lower frequencies or with inadequate filtering. This leads to diminished signal-to-noise ratios (SNR), which can markedly alter electrochemical data, especially in low-current or high-impedance contexts.

Consequently, there is a distinct necessity for a versatile, thoroughly documented, and economical potentiostat that achieves a pragmatic balance among use, precision, and cost-effectiveness. The device must perform precise cyclic voltammetry, be quickly constructed with readily available components, and be adaptable for both breadboard prototype and PCB implementations. Furthermore, it must possess an open-source structure facilitating straightforward modifications and community contributions, and be specifically designed for STEM teaching, fieldwork, and low-resource research settings.

This thesis seeks to address this deficiency by creating a microcontroller-based potentiostat utilizing the Arduino Uno platform. The design prioritizes cost effectiveness, adaptability, and replicability, focusing on applications in educational laboratories, D.I.Y. maker spaces, and small-scale analytical research. The system integrates software filtration, adjustable parameter control, and compatibility with serial data logging and graphical interfaces, thereby fulfilling both educational and technological criteria.

Chapter 3

Cyclic Voltammetry

The foundation of any electrochemical measurement is the regulated manipulation and assessment of electrical potential and current in a solution with redox-active species. The potentiostat, the primary device for electrochemical regulation, necessitates a thorough comprehension of the establishment of potentials and the driving and measurement of currents. This chapter draws substantial inspiration from the work published in [19]. Portions of the text have been adapted to maintain continuity and to explain the underlying principles more effectively.

This chapter offers a detailed examination of the electrochemical concepts pertinent to the design and functioning of a potentiostat, with particular emphasis on the roles of the three-electrode system: the working electrode (WE), reference electrode (RE), and counter electrode (CE). The text examines potentiometric and voltammetric methodologies, highlighting both theoretical and practical aspects crucial for

precise and consistent electrochemical measurements.

3.1 Electrochemistry

Electrochemistry is an important technique in the study of reactions that involve the movement of electrons. The majority of the important reactions, especially those of inorganic chemistry, are redox (reduction–oxidation) which involves one of the substances gaining electrons (reduction) while the other losing electrons (oxidation).

3.1.1 The Reduction Forces

In order to emphasize the difference between an electrochemical and chemical reduction, take the following generic case in which a cationic species A^+ is reduced to the neutral species A. In a chemical reduction, another chemical species (called a reducing agent) donates electrons to A^+.

$$A^+ + B \rightleftharpoons A + B^+.$$

Here, B provides the electrons to reduce A^+. The ability of this reaction to occur depends on the chemical nature of B . If B is a strong reducing agent, the reaction happens easily. If B is weak, the reaction may not occur at all. Importantly, to change the reaction conditions, you must change the chemical reducing agent 3.1 **A**. On the other hand in an electrochemical reduction, the electron does not come from a chemical species but from an electrode (a solid conductor like platinum, gold, or carbon). The electrode is connected to an external power source such as a

potentiostat, which supplies electrons at controlled and deterministic energies. The reaction is:

$$A^+ + e^- \rightleftharpoons A.$$

Here, the electrode surface transfers electrons directly into A^+. By adjusting the applied voltage, we control whether electrons have enough energy to reduce A^+. If the applied voltage is high enough and has the correct polarity, the reductiondoes indeed take place (Figure 3.1**B**)

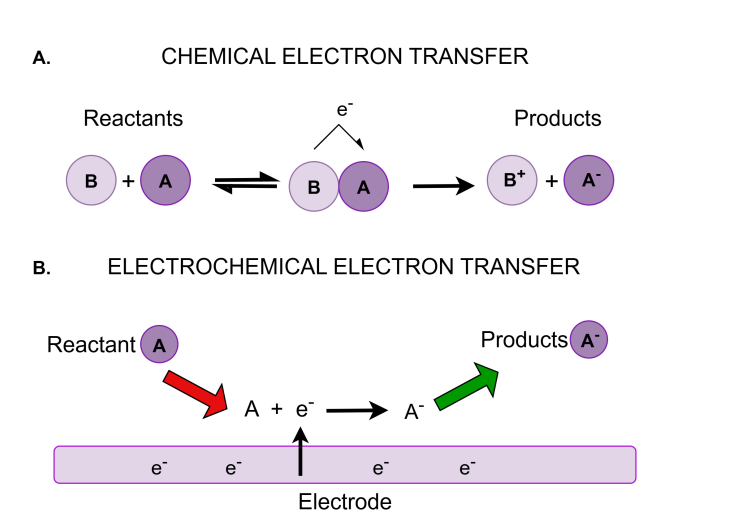

Figure 3.1: *(A) Chemical and (B) Electrochemical reduction of A^+ to A. The potentiostat controls the electrode electron energy, which can be increased until electron transfer becomes favorable.*

3.1.2 Cyclic Voltammetry and the Voltammogram

Cyclic voltammetry is a very common electrochemical technique. In this technique a voltage is applied to an electrochemical cell and the resulting current is measured. The ramp voltage is swept between a lower $-V_o$ and upper $+V_o$ limit in a cyclic

fashion. The sweep is generally as shown in Figure 3.2. It can be run once or repeatedly, depending on the desired information. The sweep is carried over a time duration at a certain sweep rate on the working electrode in a quiescent solution, and then the resulting current is measured. The sweep rate is generally adjustable. It is a powerful tool for determining the redox properties of species present in solution as well as those adsorbed on the electrode surface. Cyclic voltammetry can be described as a complex time-dependent function of a vast array of chemical and physical parameters.

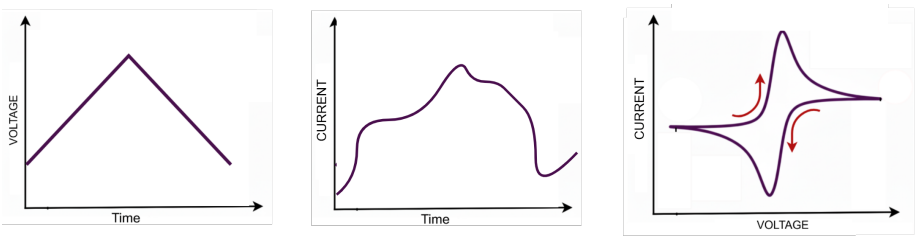

Figure 3.2: *(Left) Applied triangular voltage waveform, (Middle) Corresponding current–time response, (Right) Resulting cyclic voltammogram illustrating the electrochemical behavior of the system.*

We can plot the voltage versus current as a voltammograms, illustrated in Figure 3.3, with a more precise designation being cyclic voltammogram (CV). A typical cyclic voltammogram of the output for a quasi-reversible diffusion-controlled species has horizontal axis denoting the externally regulated variable, specifically the applied potential (E), whereas the vertical axis illustrates the system's reaction, represented by the resultant current (i) that is generated. In certain instances, the current axis may not be distinctly labeled; rather, a scale bar might be incorporated within the graph itself. Each trace is associated with an arrow to indicate the direction of the potential sweep during the data acquisition procedure.

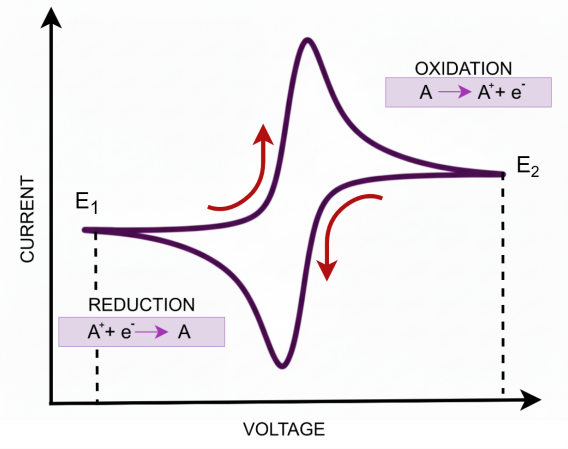

Figure 3.3: *The process of cyclic voltammetry displayed in a cyclic voltammogram .*

As depicted in Figure 3.3 , the forward scan from E_1 to E_2 is anodic trace also known as oxidation trace as it gives the oxidation peak. During the forward potential sweep (positive), the applied voltage increases from initial potential E_1 to more positive potential E_2. As the potential become more positive, the electroactive species present in solution undergoes oxidation that generates an anodic current that rises until it reaches the oxidation peak. Beyond this point, the anodic current starts to decrease. When the scan direction is reversed (negative) the potential is swept back from E_2 to E_1, and the oxidized species start reducing back to their original state producing a reduction peak showing maximum cathodic current.

3.1.3 Nernst Equation

The Nernst equation helps to predict electrochemical cell potential at any known temperature, pressure, and concentration. The equation relates the reduction potential of the cell at a non-standard condition to that of standard conditions [18].

For the electrochemically reversible electron transfer $X + e^- \rightleftharpoons X^-$, the Nernst equation is written as follows:

$$E = E^0 + \frac{RT}{nF} \ln\left(\frac{C_{X^-}}{C_X}\right) \tag{3.1}$$

where E is the electrode potential (in Volts), E^0 is the standard reduction potential of the X/X^- couple (in Volts), R is the gas constant ($8.315\,\mathrm{J\ K^{-1}mol^{-1}}$), T is the temperature (in Kelvin), n is the number of electrons transferred , and F is Faraday's constant ($96{,}485\,\mathrm{C\ mol^{-1}}$), and C_X or C_{X^-} is the concentration of the respective species (X or X^-) at the electrode.

It is important to remember that we are only concerned with the concentrations of the species at the electrode, which can differ from the concentration of the analyte in bulk solution.

While analyzing CV data electrochemical reversibility is related to kinetics for electron transfer occurring within electrode interface: fast kinetics produce sharp, peak-symmetric profiles consistent with Nernstian equilibrium; slower kinetics add additional overpotentials and widen spread between peaks. As a result, the voltammograms with peak shapes represent a direct signature of the interdependence between electrode potential, concentration gradient, diffusion phenomena, and reversibility related to redox conversion [19].

3.1.4 Impact of Scan Rate on Peak Currents and Diffusion Control

The scan rate employed in a cyclic voltammetry experiment specifies the rate with which applied potential is changed over the electrode. An increase in scan rate causes a reduction in dimensions for the diffusion layer near to the electrode surface, thereby resulting in elevated peak currents. For an electrochemically reversible electron transfer process with freely diffusing redox species, such a relationship is formulated [19] by the Randles–Sevcik equation:

$$i_p = 0.4463\, n^{3/2} F^{3/2} A C_0 D_0^{1/2} \left(\frac{\nu}{RT}\right)^{1/2}, \tag{3.2}$$

where i_p represents the peak current (A), n is the number of electrons involved in the redox process, A (cm^2) denotes the electrode surface area (commonly approximated as the geometric area), D_0 ($\mathrm{cm}^2\ \mathrm{s}^{-1}$) is the diffusion coefficient of the analyte, C_0 ($\mathrm{mol\ cm}^{-3}$) is the bulk analyte concentration, R is the universal gas constant, T is the absolute temperature, and ν ($\mathrm{V\ s}^{-1}$) represents the scan rate. According to this equation, the peak current exhibits a linear dependence on the square root of the scan rate for species undergoing purely diffusion-controlled electron transfer. This relationship not only serves as a diagnostic criterion for identifying diffusion-controlled behavior but also provides a means to determine the diffusion coefficient of the analyte.

However, deviations from such a linear relationship can yield valuable mechanis-

tic information. If a graph of i_p versus $\nu^{1/2}$ does not hold a linear relationship, then only two scenarios prevail: (a) the process of electron transfer is not fully reversible but quasi-reversible, or (b) the analyte is not fully maintained in solution but instead adsorbs to the electrode surface. Therefore, analysis of dependence of current on scan rate can be utilized to discriminate between freely diffusing and adsorbed species on a surface. Additionally to that, peak separation between anodic and cathodic peaks is one more diagnostic available: for a quasi-reversible electrolytic transfer peak-to-peak separation increases with scan rate but for an adsorbed species such a dependence is not seen. Overall, Randles–Sevcik analysis is a suitable method to determine whether an analyte is a homogeneous, diffusion-controlled entity in solution or if adsorption or kinetic limitations are involved. It is a critical distinction to make to properly interpret electrochemical reactivity and retrieve credible parameters for example a diffusion coefficient. The experimental results interpreted in light of the scan-rate analysis are discussed in section 5.4.1.

3.2 Collecting Voltammetric Data

3.2.1 Electrochemical Cell

For cyclic voltammetry (CV) experiments, an electrochemical cell is the fundamental experimental platform. An electrochemical cell used in testing D.I.Y. potentiosat for electrochemical measurements is shown in Figure 3.4. In the following account, details will be given to explain the role of each constituent part and present a logical account to assemble the cell to acquire reliable and repeatable CV measurements.

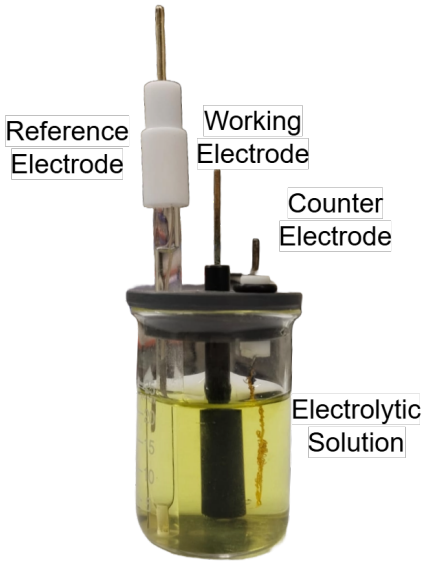

Figure 3.4: *Electrochemical setup used for testing.*

3.2.2 Preparation of the Electrolyte Solution

During a cyclic voltammetry (CV) experiment, electron transfer between analyte and electrode should be accompanied by migration of ions within solution so as to maintain electrical neutrality as well as to facilitate current flow. For convenience of such a process as well as simplification of solution resistance, a supporting electrolyte is dissolved in a solvent to form what is typically referred to as electrolyte solution.

3.2.3 Solvent

The solvent is also crucial to delivering accurate and reproducible measurements of electrolysis. An optimum solvent is one that is a liquid at experimental temperature, that dissolves the analyte and supporting electrolyte with high enough concentrations

to adequately cover solution properties, and is resistant to reduction and oxidation within the region of interest. It is also a requirement that a solvent be chemically inactive towards analyte and supporting electrolyte.

3.2.4 The Supporting Electrolyte

The supporting electrolyte ensures adequate ionic conduction and prevents unwanted analyte migration. A good supporting electrolyte should be highly soluble in the solvent being chosen, chemically and electrochemically inactive within experimental conditions, and purifiable. High electrolyte levels ensure low solution resistance with concurrent reduction of ohmic drop. Moreover, they minimize analyte migration by providing ionic conduction to the electrode interface being controlled by the electrolyte rather than by the analyte.

In reality, mass transport of species in the electrochemical cell results from convection, migration and diffusion. Convection is eliminated by not stirring or vibrating and migration is eliminated by using excess electrolyte. In conclusion, the presence of high concentration supporting electrolyte supresses analyte migration, lower solution resistances and ensure that the electrochemical response remains purely diffusion controlled.

Each solvent needs a supporting electrolyte that matches its polarity, solubility properties and electrochemical stability window for e.g., in inorganic electrochemistry, ammonium salts are commonly favored supporting electrolytes in organic solvent because they fulfill the principal requirements of solubility, stability and in-

ertness.

3.3 Electrodes

A standard three-electrode arrangement is used typically for CV experiments. In our project, a glassy carbon working electrode, a gold wire counter electrode, and an Ag^+/Ag pseudoreference electrode is used . This design isolates the function of current flow from that of potential measurement: the working electrode is where electron transfer with analyte occurs, a circuit is completed by the counter electrode carrying the balancing current, and a stable potential reference is supplied by a reference electrode from which voltages applied are measured. This arrangement schematically represented in Figure 3.5.

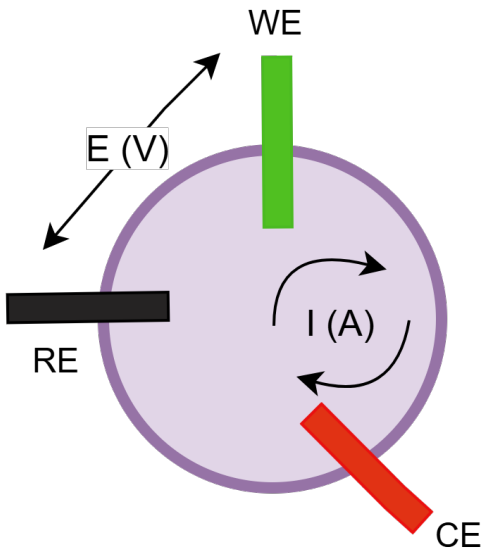

Figure 3.5: *Schematic of the three-electrode electrochemical cell, where the potentiostat controls the potential between the working and reference electrodes while measuring the current flowing between the working and counter electrodes.*

Adequate cleaning, treatment, and upkeep of electrodes are also relevant to obtaining reproducible results.

3.3.1 Working Electrode

The working electrode is where the relevant electrochemical phenomenon of interest happens. In our setup, we used a simple carbon electrode shown in Figure 3.6. It is controlled with high precision by a potentiostat and placed at potential with respect to the reference electrode. Selective investigation of redox activity is therefore possible. A basic necessity for a working electrode is that it should be made of a material that is electrochemically inactive within the investigative window of potential. The electrode material can be changed according to experimental requirements. For reproducible and reliable measurements, the surface has to be highly clean and with a definite area. Mechanical polishing is most commonly employed for preparing electrodes, especially with glassy carbon and platinum electrodes. Another variable that can significantly influence the perceived electrochemical signal is the choice of the electrode material. Variable electron-transfer kinetics, adsorptive ability, or material-specific interaction with the analyte can cause disparate voltammetric behavior. For these reasons, it is a frequently employed strategy to deploy a different electrode material to diagnose anomalous responses as well as to probe the mechanistic details of the redox events.

3.3.2 Reference Electrode

A reference electrode has a constant and unique equilibrium potential. It is a standard against which the potential of some other electrode is determined within an electrochemical cell. There are a variety of standard (and commercially available) electrode assemblies whose electrode potential is independent of the particular electrolyte being used within the cell. Some of the most commonly utilized reference electrodes utilized within aqueous media include the saturated calomel electrode (SCE), the standard hydrogen electrode (SHE), and the AgCl/Ag electrode. It is advisable to avoid junction potentials by having solvent and electrolyte within the reference compartment to be identical to that being utilized within the experiential setting. The reference electrode used for testing our D.I.Y. potentiostat is an AgCl/Ag electrode, shown in Figure 3.6 given below.

3.3.3 Counter Electrode

Once a sufficient potential is placed on the working electrode (WE) with enough ability to induce reduction or oxidation of the analyte, a current results. The counter electrode (CE) is critical to forming an overall electric circuit by providing an exchange of electrons between the WE and CE. To prevent the kinetics of the electrochemical reactions taking place within the CE from becoming a limiting factor for any reactions occurring within the WE, the counter electrode is constructed to have a significantly higher surface area than that of the working electrode. Typically, platinum wires or gold wires (Figure 3.6) are used for this; but carbon-based electrodes have also come into play for some applications.

Figure 3.6: *Experimental three-electrode used for electrochemical testing in our setup (top) Simple carbon working electrode used for testing, (centered) Gold wire used as counter soldered to a connector and (bottom) AgCl/Ag reference electrode used to maintain a constant reference potential.*

During its functioning, a reduction occurring at the WE is balanced by a related oxidation occurring at the CE. For such a counter electrode to function effectively, it has to be highly chemically and electrochemically inactive. However, side reactions or by-products might occur at the CE under some experimental conditions. To ensure such effects are reduced to a usable level, the CE might be encapsulated in a fritted compartment such that it is separated from the rest of the solution but retains the capability of ionic conduction.

3.3.4 V-I Characterization Using Electrochemical Electrodes

When a voltage is applied between the two electrodes, the potential drop between the working electrode (WE) and reference electrode (RE) is given by

$$E = \phi_m - \phi_s.$$

Here ϕ_m is the metal potential and ϕ_s is the solution potential. This difference is the driving force for electrolysis to occur. However, this potential difference is ideal for two electrode assembly (WE vs. RE) when tiny current pass through the electrodes.

Now, consider a voltage is applied between WE and RE, a large amount of current starts to flow between these electrodes. Then the potential difference is described as;

$$E = (\phi_m - \phi_s) + iR + (\phi_s - \phi_{REF}) \tag{3.3}$$

where iR is voltage drop in solution due to large current, R is the electrical resistance and $(\phi_s - \phi_{REF})$ is potential drop at RE which is fixed by the chemical composition of chosen RE. As we know, the aim of voltammetry experiment is to measure i as the function of $(\phi_m - \phi_s)$. For small current the term iR is negligible and $(\phi_s - \phi_{REF})$ is constant , eq (3.3) simplifies in to

$$E = \phi_m - \phi_s + constant.$$

With large current the iR is not negligible and it also affects the chemical composition of the reference electrode, so to overcome this problem the third electrode (Counter Electrode) is deployed in the electrode assembly. These processes are driven by the potentiostat (Figure 3.5), which ensures that current flows only between the working electrode WE and the counter electrode CE. The potential of the working electrode is maintained constant with respect to a stable reference electrode RE, and the electronic circuitry is designed to prevent any current from flowing through the

reference electrode branch of the circuit [20].

3.3.5 Peak-Shaped Cyclic Voltammogram

CV provides simultaneous information on both oxidation and reduction behaviour of an electrochemical specie and is widely used for the investigation of electron-transfer kinetics, reversibility and coupled chemical reaction.

Consider an experiment is conducted in stationary solution under this condition mass transport occurs exclusively via molecular diffusion, driven solely by concentration gradient, without interference from mechanical stiring or convection. Diffusion arises from the random thermal motion of molecules and leads to net movement from region of high concentration to region of low concentration. This process is quantitatively described by Fick's laws of diffusion. For electrochemical systems operating under non-steady-state conditions, the diffusion behaviour is explained by Fick's second law

$$\frac{\partial A}{\partial t} = D_A \frac{\partial^2 A}{\partial x^2}, \tag{3.4}$$

which describes how the concentration of a specie changes with time as a result of diffusion.

In cyclic voltammetry, the applied potential varies continuously with time, causing the concentration of electroactive species at the electrode surface to deviate from its bulk value. This perturbation leads to the formation of a diffusion layer whose thickness increases with time as species diffuse between the electrode surface and the bulk solution. The redistribution of species within this transient diffusion layer

is governed entirely by Fick's second law. The resulting current response reflects the time-dependent concentration gradient at the electrode interface, and the rise and decay of current during the forward and reverse potential scans originate from the progressive development and relaxation of these diffusion-controlled concentration profiles. Consequently, the characteristic shape of the cyclic voltammogram is a direct manifestation of the diffusion process described by Fick's second law.

The duck-shaped voltammogram shown in Figure 3.7 arises from the time dependent evolution of concentration gradient during cyclic potential sweep, when the potential sweep is initiated from negative values, the applied potential is insufficient to drive electron transfer and the electro-active species remains uniformly distributed throughout the solution, including at the electrode surface, corresponding to region (**a**) of the voltammogram. Under these conditions, no significant faradaic current is observed because no concentration gradient exists to induce diffusive flux. As the potential is swept in the positive direction, the driving force for oxidation increases and electron transfer of to form begins at the electrode surface, marking the onset of current rise at point (**b**). During this stage, the surface concentration of decreases while the bulk concentration remains essentially unchanged, resulting in the establishment of a concentration gradient normal to the electrode surface. The resulting current is governed by the diffusive flux of, which is proportional to the concentration gradient at the interface, while the surface concentrations are maintained by fast reversible electron-transfer kinetics described by the Nernst equation.

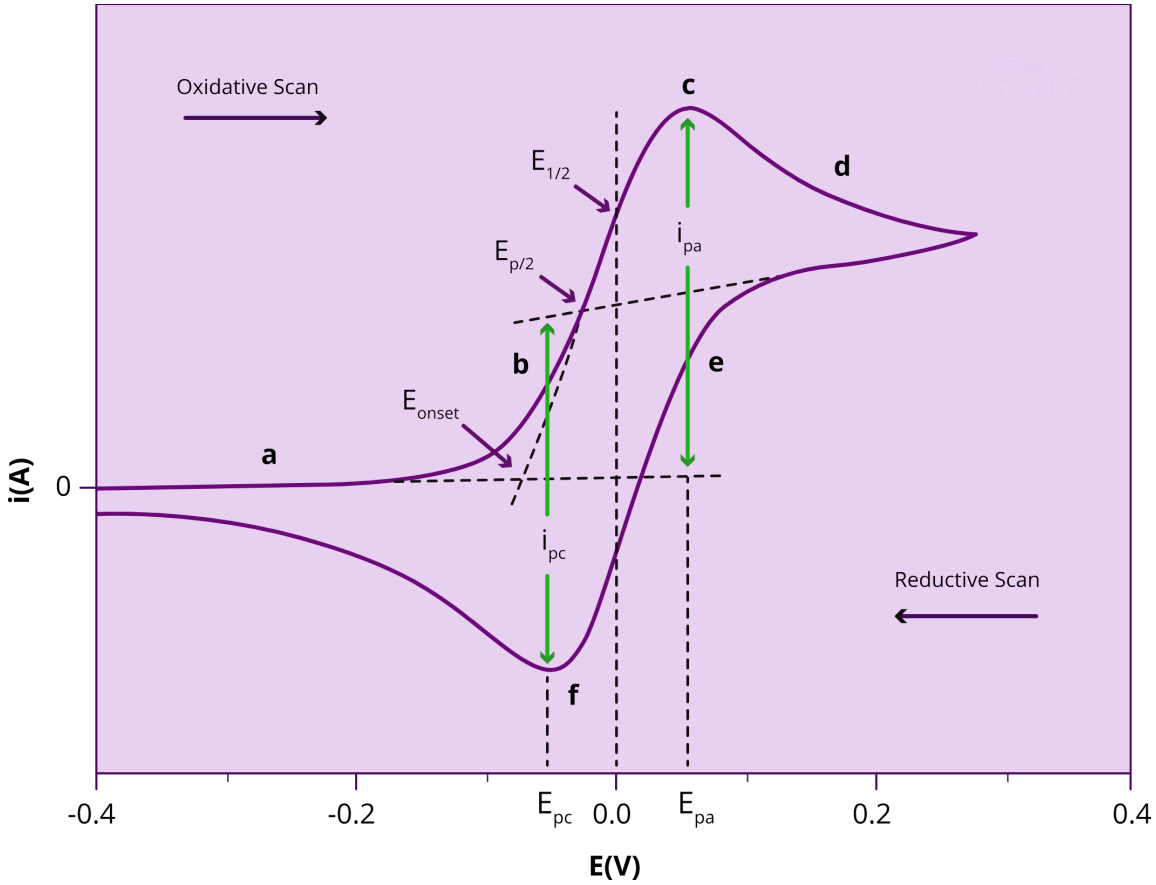

Figure 3.7: *Duck-shaped voltammogram showing the oxidation and reduction peaks.*

As the potential continues to increase, the rate of oxidation becomes sufficiently high that the surface concentration of approaches zero, and the current reaches a maximum at point (**c**), defined as the anodic peak current at the anodic peak potential. At this point, the current is entirely limited by mass transport, as the flux of to the electrode is controlled by diffusion through a growing diffusion layer whose thickness increases with time in accordance with Fick's second law. Beyond the anodic peak, although the applied potential continues to increase, the current de-

creases, as shown in region (**d**), because continued electrolysis further depletes near the electrode and the diffusion layer becomes progressively thicker, reducing the concentration gradient and hence the diffusive flux. Upon reversing the potential sweep, the accumulated oxidized species present within the diffusion layer is reduced back to, giving rise to an increasing cathodic current in region (**e**). Initially, the high local concentration of near the electrode produces a steep concentration gradient, resulting in a rapid increase in reduction current. As the reverse scan proceeds, the surface concentration of decreases due to reduction, and a cathodic peak current is observed at point (**f**), corresponding to the cathodic peak potential . Further progression of the scan leads to depletion of within the diffusion layer and a consequent decay of the current toward zero. For a reversible redox system under diffusion control, the anodic and cathodic peak currents are equal in magnitude, and the overall peak-shaped or duck-shaped voltammogram reflects the time-dependent evolution of concentration gradients at the electrode solution interface, governed fundamentally by Fickian diffusion during the potential sweep.

3.3.6 Practical Considerations for the Electrochemical Cell

In electrochemical measurements, numerous factors affect accuracy and reliability. A critical factor is the stability of the reference electrode. The reference electrode must demonstrate non-polarizable properties and be shielded from current flow. Any disruption in its potential such as from the evaporation of the internal electrolyte or obstruction at the liquid junction can result in artefacts in voltage regulation and monitoring.

An additional significant aspect is the ohmic drop (IR drop), which occurs due to resistance within the solution or electrical connections. According to Ohm's Law, this resistance results in a voltage drop, indicating that the actual potential at the working electrode may deviate from the value set by the potentiostat. This disparity can skew voltammetric results, particularly at elevated currents. To mitigate these effects, researchers frequently employ high- conductivity supporting electrolytes and implement IR compensation strategies. Electrochemical systems necessitate high impedance measurement, especially in potentiometric configurations. Voltmeters possessing elevated internal resistance are essential to guarantee that the measurement procedure extracts minimal current, hence averting alterations in the measured potential attributable to the measuring instrument itself.

Finally the arrangement and placement of the electrodes are also essential. Correct alignment and spacing among the working, reference, and counter electrodes mitigate measurement inaccuracies. The implementation of a Luggin capillary which situates the reference electrode in proximity to the working electrode, significantly reduces the impact of solution resistance on the measured potential. We must keep in mind that materials utilized for electrodes substantially also influence system performance. The working electrode (WE) typically consists of inert conductive elements such as platinum, gold, or carbon, frequently enveloped in insulating sheaths to delineate specific active surface areas. The counter electrode (CE) is generally larger and composed of comparably inert materials, ensuring it can endure current flow without considerable polarization, thereby preserving system stability throughout operation.

3.4 Electrode Maintenance and Preparation

The reliability of potentiostat-based electrochemical measurements depends strongly on the condition of the electrodes used in the three-electrode configuration. Inadequate cleaning, improper storage, or surface degradation of the reference, counter, or working electrode can introduce potential instability, signal drift, and poor reproducibility. This section outlines standardized procedures for electrode maintenance and restoration to ensure stable and consistent electrochemical performance.

3.4.1 Restoration of Reference Electrodes

Reference electrodes provide a stable potential and must be maintained in a hydrated and chemically equilibrated state. For aqueous systems, the electrode junction must always remain immersed in potassium chloride (KCl) solution to preserve ionic conductivity across the porous frit. Drying of the junction leads to salt crystallization and increased junction resistance, which manifests as unstable reference potentials.

During storage, the electrode tip is kept wetted in KCl solution, preferably using the manufacturer-provided storage bottle containing a saturated sponge. For short durations, immersion in an external container filled with KCl solution is acceptable. Restoration of the reference electrode involves periodic replacement of the outer filling solution. The depleted electrolyte is removed, the chamber is rinsed with ultrapure water or fresh KCl solution, and the electrode is refilled to a level slightly below the cap to maintain proper pressure conditions. In double-junction electrodes, restoration is limited to replacement of the outer KCl solution.

If junction blockage occurs, the frit can be restored by soaking in KCl solution or ultrapure water, with mild heating used if necessary to dissolve salt deposits. Care must be taken to avoid electrolyte combinations that form insoluble precipitates, as these can permanently obstruct the junction.

3.4.2 Cleaning of Counter Electrodes

The counter electrode is required to sustain current flow without participating in the electrochemical reaction. Maintenance is therefore focused on cleanliness and mechanical integrity. After use, residual electrolyte is removed and the electrode is rinsed thoroughly. For non-aqueous systems, rinsing with the same solvent is necessary to prevent residue formation. The isolation tube is cleaned concurrently to ensure unrestricted ionic communication through the frit.

For storage, the electrode is kept within its glass isolation tube to protect the coils from deformation. Once cleaned, dry storage is sufficient and does not compromise performance.

3.4.3 Polishing and Resurfacing of Working Electrode

The electrochemical response is most sensitive to the surface condition of the working electrode, as electron transfer occurs directly at this interface. Routine surface restoration is performed by polishing the electrode on a micro-cloth pad using a fine alumina slurry. During polishing, the electrode surface is held parallel to the pad and moved in a controlled figure-of-eight (8-sign) motion, which ensures uniform

abrasion across the entire surface and prevents preferential wear in a single direction. This step removes adsorbed species and restores a reproducible and smooth electrode surface.

Periodic polishing employs a slightly coarser alumina suspension to remove more persistent surface films that accumulate after repeated measurements. This procedure is followed by fine polishing to re-establish a uniform surface finish. After each polishing step, the electrode must be thoroughly rinsed with distilled or ultrapure water to remove residual alumina particles, as trapped abrasives can interfere with charge transfer. Brief ultrasonic cleaning of only the electrode surface may be used to enhance particle removal.

When routine and periodic polishing do not recover stable electrochemical behavior, aggressive cleaning may be applied using coarse alumina on a nylon polishing pad. In cases of severe surface damage, complete repolishing with silicon carbide paper can be performed; however, this process removes a substantial amount of electrode material and significantly reduces electrode lifetime. Repeated complete repolishing eventually exposes the underlying substrate, at which point the electrode becomes unsuitable for further use.

Chapter 4

Circuit Design and Integration

This chapter outlines the practical execution of the Arduino-based potentiostat circuit engineered for conducting electrochemical experiment utilising a three-electrode configuration with the typical intent to perform CV. This chapter, based on the theoretical foundation established in previous chapter, examines the practical implementation of the design, analysing the functions of individual components, the circuit topology and the hardware layout. The design prioritises cost-efficiency, simplicity, adaptability, and accuracy, facilitating its application in voltammetric studies.

For conversion of theoretical constructs of electrochemistry to quantifiable results, selective equipment is needed. As described earlier the basis for essentially all current electrochemical measurements is the potentiostat. A potentiostat is an electronic instrument designed to control the potential of a working electrode (WE) relative to a reference electrode (RE) while simultaneously measuring the current

that flows between the working and counter electrodes (CE). By virtue of its dual operation, the potentiostat is tasked with investigation of electron transfer reactions, creation of cyclic voltammograms, and exact quantification of redox-active species.

4.1 Operational Overview of the Potentiostat System

Figure 4.1 illustrates the basic components and operation of a potentiostat. The system is first activated through a computer, which controls the device via dedicated software. The input instructions (green arrow) are sent to the potentiostat and received by the microcontroller, which functions as the central control unit of the device.

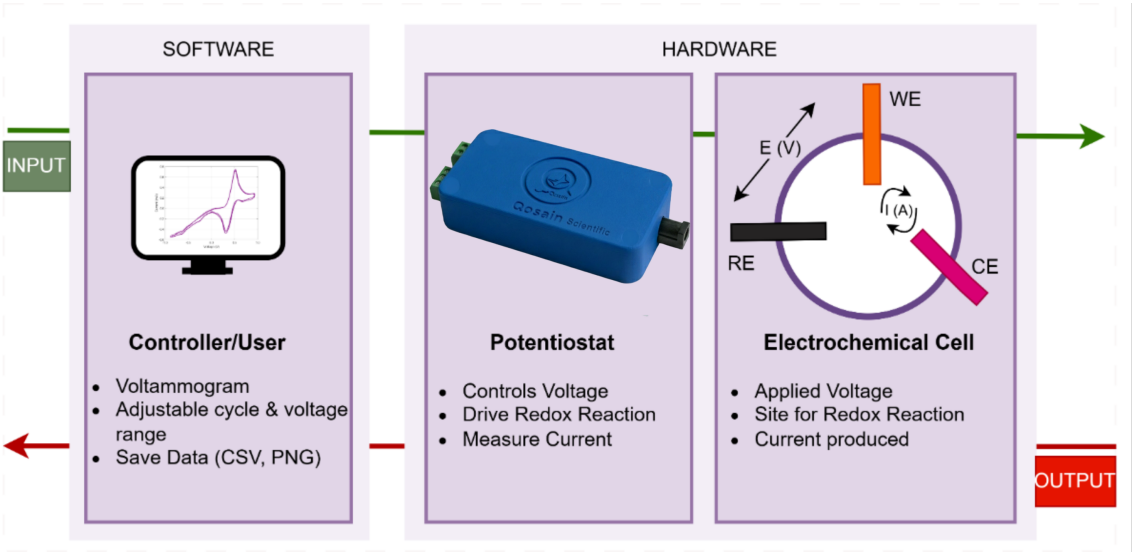

Figure 4.1: *Schematic representation of a potentiostat and its operation, showing the flow from the controller to the electrochemical cell. The input signal is indicated by the green arrow, while the output response is shown by the red arrow.*

The microcontroller converts the digital control signals into analog outputs using the digital-to-analog converter (DAC). These analog signals are then delivered to the electrode interface circuit, which drives and regulates the three electrodes of the electrochemical cell. After an electrochemical method is applied, the potentiostat sets and maintains the potential difference (E) between the working electrode (WE) and the reference electrode (RE), while simultaneously measuring the resulting current (I) flowing between the WE and the counter electrode (CE).

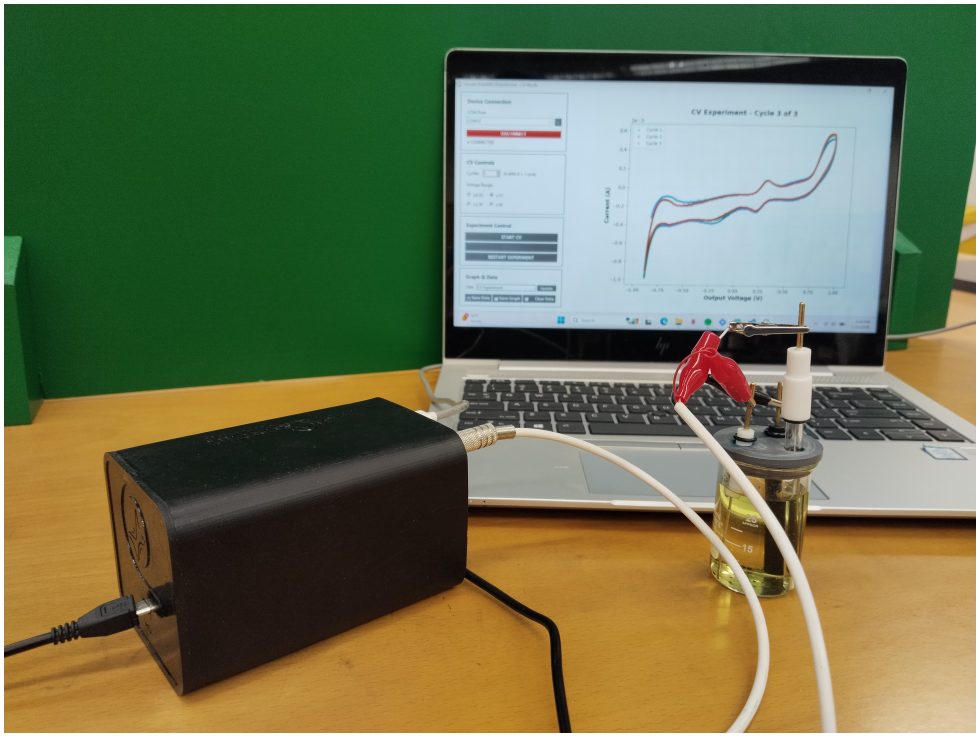

Figure 4.2: *Experimental setup for electrochemical techniques using a D.I.Y.potentiostat connected to a laptop and a three-electrode electrochemical cell.*

The measured current and potential values travel back to the potentiostat (red arrow) as analog signals. These signals first pass through the electrode circuits

and are then converted back into digital form by the analog-to-digital converter (ADC). Once digitized, the data are processed by the microcontroller and sent to the computer, where the user can view, record, and analyze the electrochemical response. The experimental setup shown in Figure 4.2 was fully designed and assembled as part of this research work.

4.2 System Architecture

The complete circuit is designed to perform two primary tasks: to provide the desired voltage range for the system controlling the potential difference (PD) while accurately measuring the resulting electrochemical current. To achieve this, as shown in Figure 4.3 potentiostat circuit is divided into five (5) functional blocks.

The Arduino alone cannot produce a smooth analog ramp signal; instead, it generates a PWM-based square wave. Therefore, the first block of the circuit converts this PWM signal into a stable and continuous potential ramp suitable for electrochemical measurements.The second block addresses the need to vary the applied potential across both negative and positive values. Thus, this part is designed to provide a controlled and useful voltage range, enabling consistent and adjustable potential steps during operation. The third block functions as the control unit. Its role is to ensure that the correct potentials are applied to the working and reference electrodes, maintaining the stability and accuracy required for electrochemical experiments. Finally, the current generated at the working electrode must be measured and translated into a voltage that the Arduino can interpret. To achieve this,

a dedicated current-to-voltage conversion (block 4) and protection circuit (block5) is included. This ensures that the Arduino receives safe, readable, and reliable voltage signals corresponding to the electrochemical current.

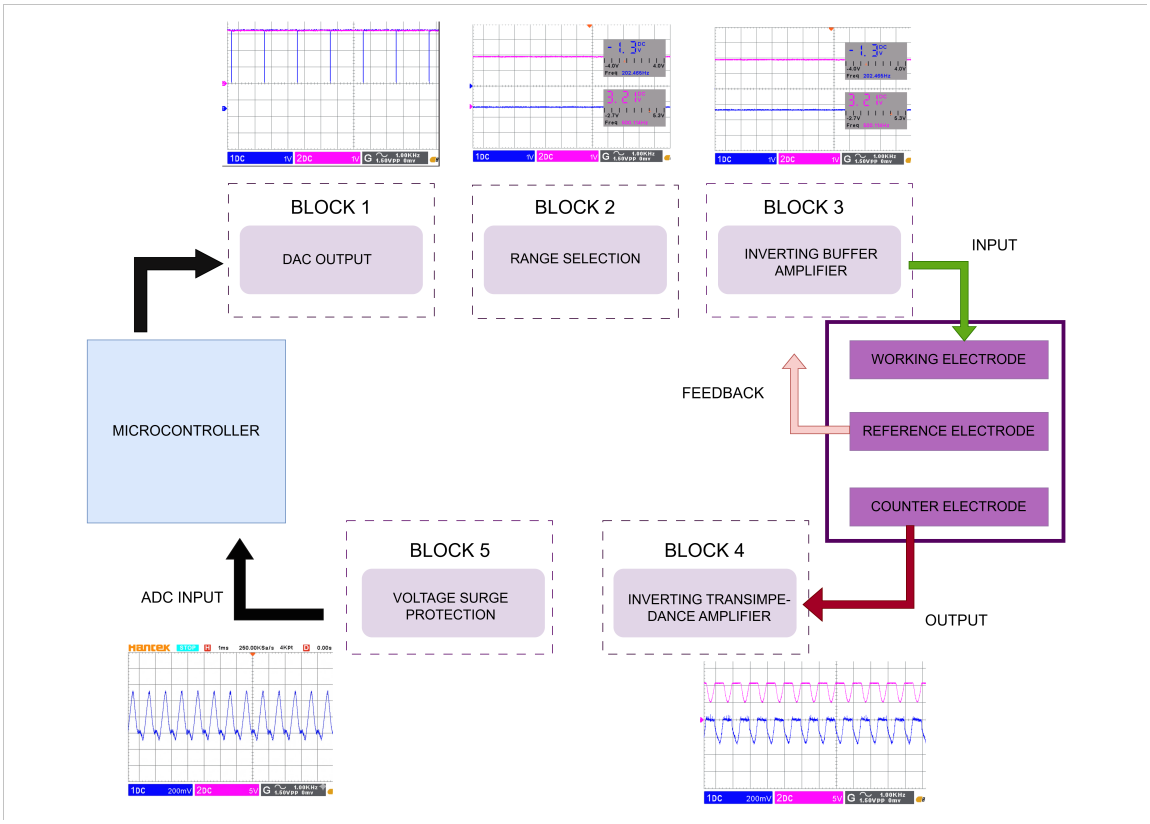

Figure 4.3: *Schematic representation of the potentiostat featuring the DAC-driven voltage regulation, current measurement circuitry, electrode interconnections, and signal processing at each point of the circuit.The input signal is indicated by blue whereas the pink colour indicates the output of block.*

4.3 Instrument Developement

4.3.1 Potentiostat Circuit and Components

The functional blocks are visually organized in the circuit diagram presented in Figure 4.4, with relevant electronic components listed in Table 4.1. The placement of every resistor, capacitor, and amplifier is based on what best supports the electrical role of that block in attaining stable operation, low noise, and compatibility with the Arduino Due control signal.

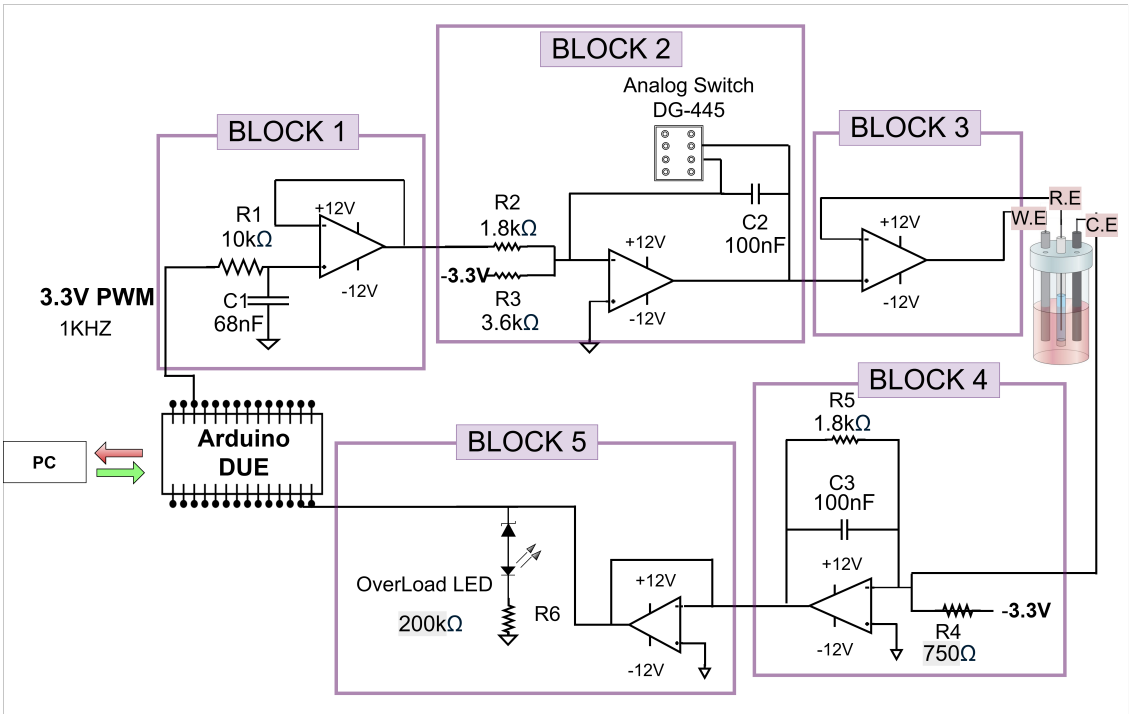

Figure 4.4: *Circuit diagram of custom built microcontroller based potentiostat.*

The analogue circuitry is energised by a symmetric ±12 V dual power supply to facilitate the bipolar output swing necessary for the operational amplifiers and the

Component Type	Function
Operational Amplifier *(TL084CN, LM324CN)*	Voltage control and current measurement
Microcontroller *(Arduino DUE)*	Digital control and data acquisition
Resistors	Gain setting, filtering
Capacitors	Filtering, stability
Zener Diode	Input protection
LED	Visual status indicator
Power Supply	Provides biasing for op-amps and analog circuitry
Electrochemical Cell	Interface with electrolyte
DG-445 Quad CMOS Analog switch IC	Varies resistance without mechanical movement

Table 4.1: *List of major components and their functions.*

electrochemical interface. The 3.3 V PWM signal is being generated by the Arduino Due, which is employed as both a 12-bit ADC and a DAC for digital to analog and analog to digital signal conversion within the circuit. The Arduino Due was selected as the controller to generate stable voltage waveforms and acquire measurement data because of its high-resolution PWM capability and built in DAC channels. To convert the pulse-width modulation into an analog voltage specific values of RC filter were chosen to achieve a cutoff frequency suitable for a 1 KHz PWM. These resistor values in circuit were selected to achieve a controlled gain while maintaining low noise. An analog switch IC is included in the feedback path to allow programmable gain adjustment, enabling flexible control of the applied potential without mechanical trimmers. The amplified control voltage is passed to a high current op-amp configured to drive

the working electrode (WE) while referencing the potential against a stable reference electrode (RE). The electrochemical current is converted into a measurable voltage using a transimpedance amplifier (TIA). To prevent op-amp saturation or excessive cell current, an overload detection circuit is implemented using a comparator and an LED indicator.

4.4 Circuit Analysis

Each block is examined in detail below, first with the Arduino-based voltage regulation and concluding with signal acquisition.

4.4.1 Digital to Analog Converter

To produce a specific voltage, the onboard DAC (digital to analog converter) of the Arduino DUE is configured for a 12-bit operation. The part exists with a limited voltage range for which the whole range gets divided by the number of the bits, which is resolution of the DAC as shown in Figure 4.5. For instance, the DAC used in our circuit has a full scale output voltage up to 3.3 V and has 12 bits which creates a resolution in a way:

$$\Delta V = \frac{3.3}{2^{12}} = \frac{3.3}{4096} \approx 8.06 \times 10^{-4}\,\mathrm{V}\ (0.806\,\mathrm{mV}).$$

This voltage variation it is also commonly called the LSB (least significant bit). As the component is digital, it cannot supply continuous voltages from $0V$ to $3.3V$. Rather it furnishes every possible voltage step on the form $N \times \Delta V$ where the

maximum value of $N = 4096 - 1$.

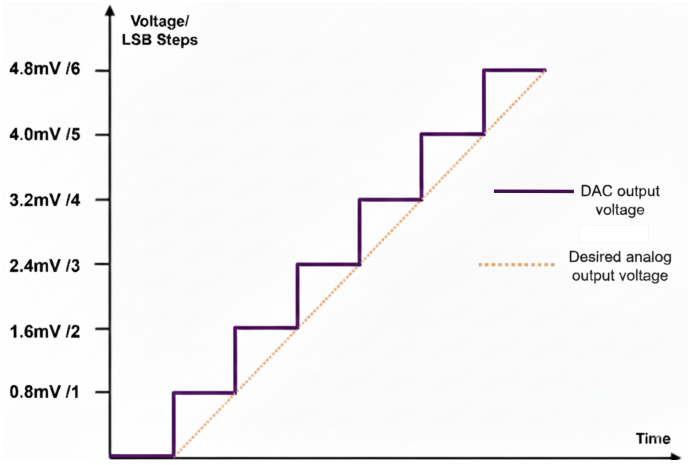

Figure 4.5: *Difference between the output voltage from an 12-bit DAC and an analog signal.*

4.4.2 Block 1: Conversion of PWM to Analogue Voltage

The Arduino produces a 3.1 KHz PWM signal with a duty cycle regulated by programming. The digital waveform is passed through a passive low-pass filter (R_1 and C_1) to generate a stable DC analogue voltage. The operational principle of a low-pass RC filter involves the attenuation of high-frequency PWM harmonics while producing an average voltage output over time. The cutoff frequency is defined as:

$$f_c = \frac{1}{2\pi R_1 C_1} \tag{4.1}$$

where $R_1 = 10\ \text{k}\Omega$ and $C_1 = 68$ nF, yielding f_c=234 Hz which is adequate for filtering the 1 KHz PWM signal.

A PWM signal is a square wave that toggles between 0-3.3 V, its duty cycles

determine its average voltage and limits the flow of current in capacitor. The capacitor charge when the PWM signal is high and discharge when it is low. If the PWM frequency is high relative to the $\tau = R_i \cdot C_i$, the capacitor does not have time to fully charge or discharge during one cycle. Instead, it smooths out the rapid changes, and output appears as a smooth. The voltage across the capacitor settles at a point that is approximately equal to the average value of the PWM waveform. (i.e. the max.voltage x dutycycle). This averaging effect converts the pulsating PWM into smooth DC voltage. The resultant DC voltage is sent to the non-inverting termi-

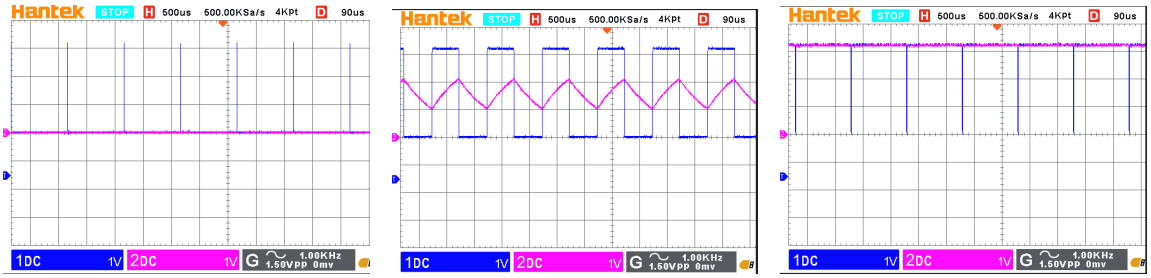

(a) *PWM signal at* **0**% (b) *PWMsignal at* **50**% (c) *PWM signal at* **100**%

Figure 4.6: *RC Filter Conversion of PWM to Sawtooth/Ramp.Waveforms show a Width Modulated (PWM) signal at different duty cycles being integrated by an RC low-pass filter to generate a sawtooth/ramp-like voltage for solution measurements. Th input signal is indicated by blue whereas the pink colour indicates the output of block.*

nal of the initial opamp inside the block 1, this op amp is a buffer it ensures the provision of drive current. If this will be absent and if the next stage has a low input impedance, significant current will be drawn from the capacitor. This will alter capacitor discharge rate and the RC filter will become ineffective. The opamp has high input impedance, which means it discharges practically zero current from the capacitor. The input and output signal of block 1 is given in Figure 4.6

4.4.3 Block 2: Signal Conditioning Amplifier

Block 2 is used to scale and level-shift the analog voltage obtained from the PWM filtering stage so that the final output voltage sweeps over the required potential window. The filtered PWM signal obtained from Block 1 is unipolar, varying between 0 V and 3.3 V. However, the target application requires a bipolar voltage sweep centered around a defined reference level. Therefore, simple amplification alone is insufficient, and level shifting must be introduced. This block is implemented using an operational amplifier configured as an inverting summing amplifier. One input of the summing amplifier receives the filtered PWM voltage, while a second input receives a fixed DC reference of -3.3 V. The non-inverting terminal of the op-amp is connected to ground, creating a virtual ground at the inverting input. Applying Kirchhoff's current law at the inverting node, the sum of currents through the input resistors must be zero. Using Ohm's law, the output voltage is given by:

$$V_{\text{out}} = -R_f \left(\frac{V_1}{R_1} + \frac{V_2}{R_2} \right).$$

Figure 4.7, the width of the window can be adjusted by changing the values of V_1, R_1, V_2, R_2, and R_f. The inclusion of the -3.3 V reference introduces a controlled DC offset at the output. This offset shifts the entire voltage sweep downward, thereby enabling the output to span both negative and positive voltage regions. Without this reference voltage, the output would remain strictly unipolar and unsuitable for applications requiring bipolar operation. The sweep range of the output voltage is determined by the resistor ratios R_1/R_f and R_2/R_f. By selecting appropriate resistor

values, the amplitude of the PWM-derived signal and the magnitude of the DC offset can be independently adjusted. This allows precise control over both the width and position of the voltage sweep window. In this implementation, DG-445 Quad CMOS Analog switch IC is used in place of a R_f allowing multiple sweep ranges to be selected and providing a wider operating window for the circuit instead of a single predefined range and ensures stable operation during measurements. A capacitor C_2 is added at the output to suppress high-frequency components and residual PWM ripple, ensuring a smooth and continuous output voltage.

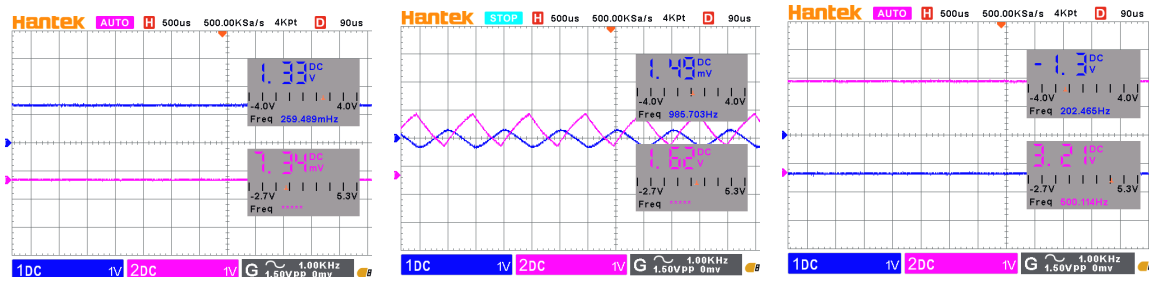

(a) *dutycycle* **0**% (b) *dutycycle* **50**% (c) *dutycycle* **100**%

Figure 4.7: *All three signals are amplified and level-shifted so that the final conditioned waveform spans* -1.5 *V to* $+1.5$ *V.Th input signal is indicated by blue whereas the pink colour indicates the output of block.*

4.4.4 Block 3: Buffering and Feedback Regulation

The amplifier's output is sent through a voltage follower (unity-gain operational amplifier). This stage guarantees elevated input impedance and diminished output impedance to operate the electrochemical cell.

Within this circuit, the voltage follower preserves the voltage at the reference electrode while enabling the operational amplifier to modify the counter electrode

potential to equilibrate the impedance of the electrochemical cell. The counter electrode (CE) is activated by the buffer output, while the reference electrode (RE) is connected to the feedback network of the operational amplifier (opamp). This configuration forces the RE to align and latch itself with the command potential, thereby completing the potentiostatic feedback loop.

4.4.5 Block4: Transimpedance Amplifier (Current Measurement)

A transimpedance amplifier (TIA) is employed to monitor the electrochemical current at the working electrode (WE). The working principle of The TIA transforms the small current from the WE into a voltage using the feedback resistor usin the relation:

$$V_{\text{out}} = -I_{\text{in}} R_6. \tag{4.2}$$

The resistor $R_6 = 1.8$ kΩ was selected to convert currents into a voltage range of ± 10 V as shown in Figure 4.8. A parallel capacitor $C_3 = 100$ nF was incorporated to mitigate high-frequency oscillations and to define a bandwidth suitable for voltammetric applications, with a cut-off frequency around 1 KHz. The resulting output is directly fed into the Arduino's analog input port for digitization after some safety checks.

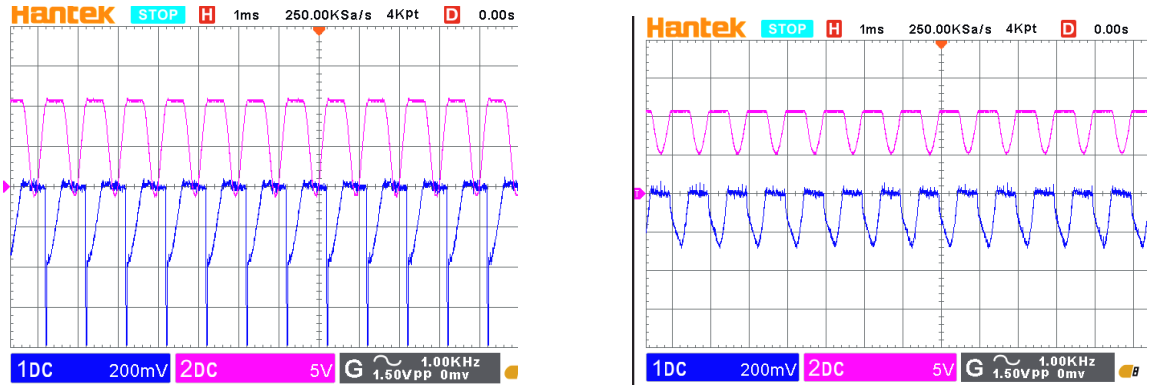

Figure 4.8: *Waveform of output signals from TIA.Th input signal is indicated by blue whereas the pink colour indicates the output of block.*

4.4.6 Block5: Saftey Circuit

To avert damage to the Arduino from overvoltage at the TIA output, a 5.1 V zener diode is positioned in parallel with an LED and a current-limiting resistor. The operational principle is that if the output of the operational amplifier exceeds 5.1 V, the Zener diode becomes active and clamps the voltage to a safe level. At the same time, the LED turns on, providing a visible indication of an overload condition. A 200 KΩ resistor is used to limit the current flowing through both the LED and the Zener diode. This protection mechanism ensures that the Arduino remains safely within its 3.3 V operating voltage limit.

4.4.7 ADC to Digital Conversion

The component used to sample the measured current, or more precisely the current transformed to voltage, is an ADC (Analog to Digital Converter). ADCs work similarly as a DAC, but instead of transforming a digital signal to an analog signal, the

ADC transforms an analog signal to a digital signal.

4.5 Hardware System Integration

4.5.1 Breadboard Prototyping

Preliminary validation was conducted on a solderless breadboard that can be seen in Figure 4.9. At this point we were using a ceramic resistor instead of digital potentiometer, it was incorperated later. Each block was fabricated and evaluated separately using the electrochemical cell. This step facilitated the iterative adjustment of component values.

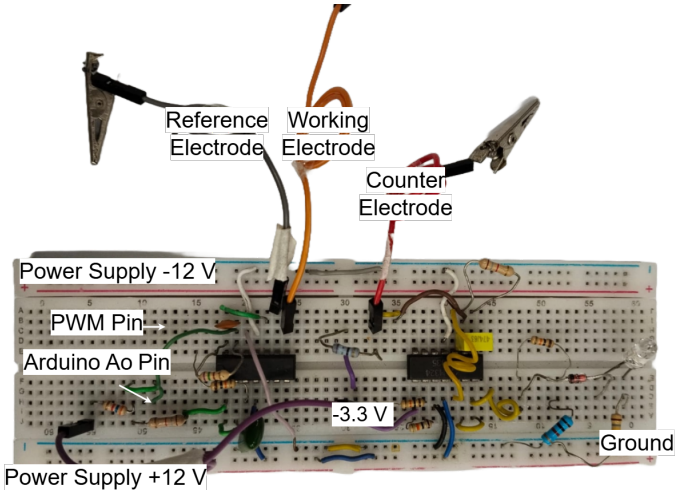

Figure 4.9: *Breadboard setup of potentiostat showing the assembled components and interconnections used for testing and verification.*

4.5.2 PCB Design Utilising EasyEDA

The final design was translated to a printed circuit board (PCB) to guarantee reproducibility and signal integrity and is displayed in Figure 4.5.2. The layout was created via EasyEDA, incorporating the subsequent considerations of isolating analogue and digital ground planes and modular connectors for interfacing the circuit with the electrochemical cell. The final PCB was assembled manually. It is small and engineered for future expansion to accommodate more electrode channels or incorporates more intricate voltammetric and electrochemical methods.

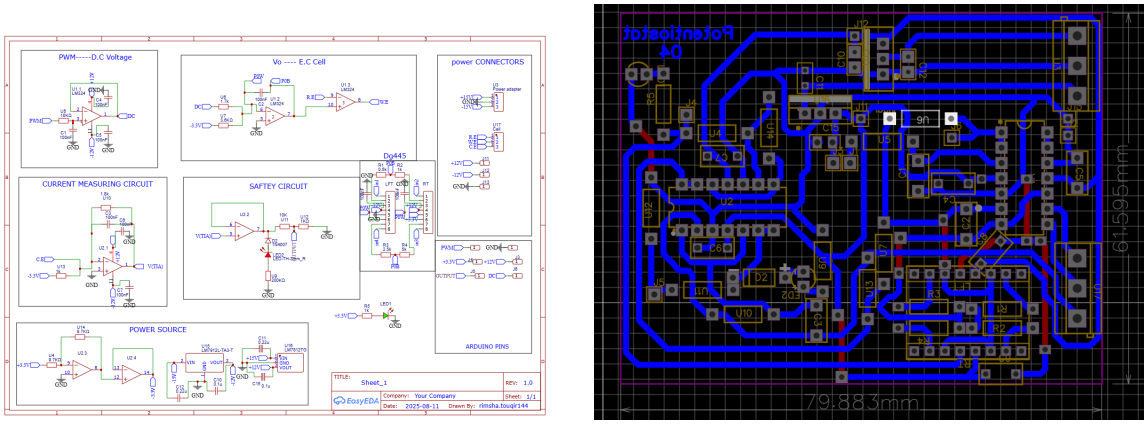

Figure 4.10: *Left: Complete schematic diagram of the potentiostat system. Right: Corresponding PCB layout showing component placement and routing.*

4.6 Software Development

The software development of the potentiostat system advanced through several phases, transitioning from basic serial connection to a comprehensive graphical interface. The core of the system is the Arduino DUE microcontroller, programmed

with the Arduino IDE in C/C++. The firmware generated the voltage waveform necessary for cyclic voltammetry, the program executed a triangle voltage sweep, incrementally altering the PWM duty cycle to facilitate forward and reverse scans with regulated time and recorded the accompanying current response from the electrochemical cell.

4.6.1 Arduino Programming

The Arduino code was designed to generate PWM signals, acquire analog data, control direction reversal of the sweep, and facilitate efficient serial communication.

4.6.2 Plotting in Jupyter Notebook

The Jupyter Notebook utilized the pyserial package to connect with the Arduino and retrieve incoming serial data. The matplotlib library was utilized to graph current against voltage in real time. This configuration facilitated a practical environment for instantaneous visualization and rapid validation.

Although Jupyter Notebook was effective for prototyping, its deficiency in user interface components and data management capabilities rendered it inappropriate for actual, user-centric experimentation. A Python GUI was created to address these restrictions by providing real-time control, noise filtration, and data export capabilities in an accessible way.

4.6.3 Graphical User Interface in Python

The Python graphical user application encompassed functionalities such as serial port identification, real-time charting, automatic cycle termination, and CSV data logging. It facilitated intuitive interaction with the potentiostat system, allowing for the execution of controlled tests with minimal exertion. The visual aesthetics and layout design rendered the interface accessible and userfriendly and is shown in Figure 4.11.

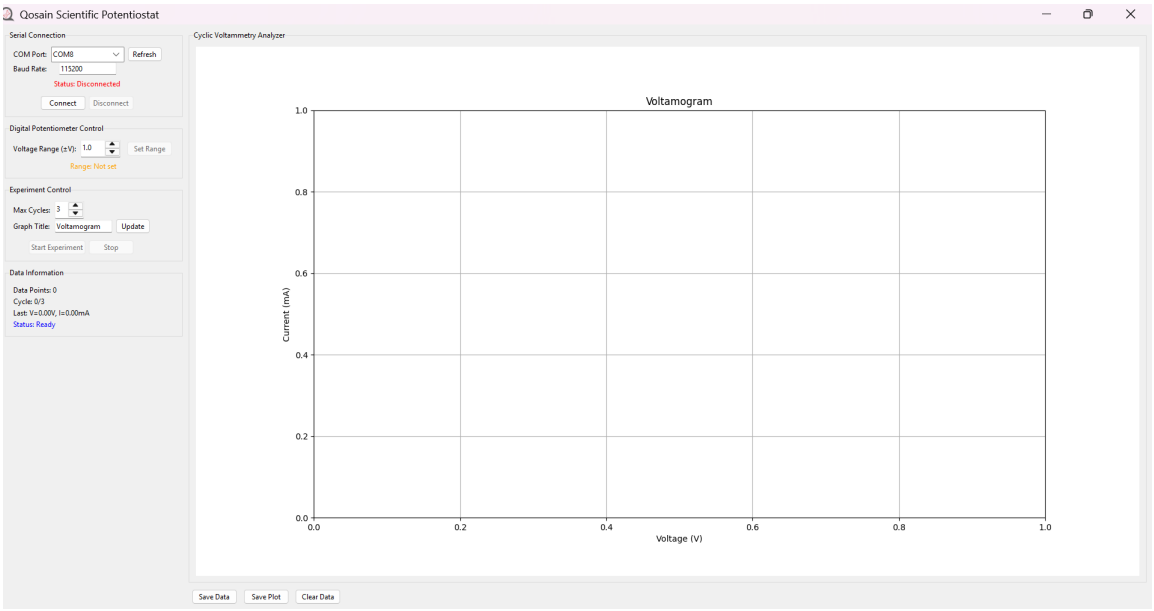

Figure 4.11: *Python-based GUI for real-time cyclic voltammetry . The interface features COM port selection, start/stop controls, real-time plotting of multiple CV cycles, user-directed data storing, and options for clearing plots.*

The shift from embedded Arduino code to Jupyter-based visualization and ultimately to a robust Python GUI markedly improved the system's dependability, repeatability, user-friendly and usefulness. The firmware and software infrastructure

facilitated precise voltage regulation, accurate current measurement, and real-time visual feedback essential functionalities for an operational and efficient potentiostat. These resources are avaliable from our website https://physlab.org/.

Chapter 5

Experimental Setup and Results

This chapter highlights the practical factors involved in conducting electrochemical experiments. It begins with the preparation of supporting electrolytes as well as the assembly of the electrochemical cell, the chapter discusses the procedure of connecting and calibrating the potentiostat to obtain reliable operation. At each step, delicacy in methodology as well as safety is stressed in order to provide consistent as well as reproducible measurement. Finally, the chapter presents the result obtained side by side with a thorough discussion correlating the experimental set up with observed electrochemical phenomena.

5.1 Practical Execution of the Experiment

5.1.1 Prepertion of Solution

The first part of the experimental process was the preparation of the electrolyte solutions. Figure 5.1 shows the process followed for the preparation of a 1 M solution of KOH, which was used as the supporting electrolyte in the electrochemical cell.

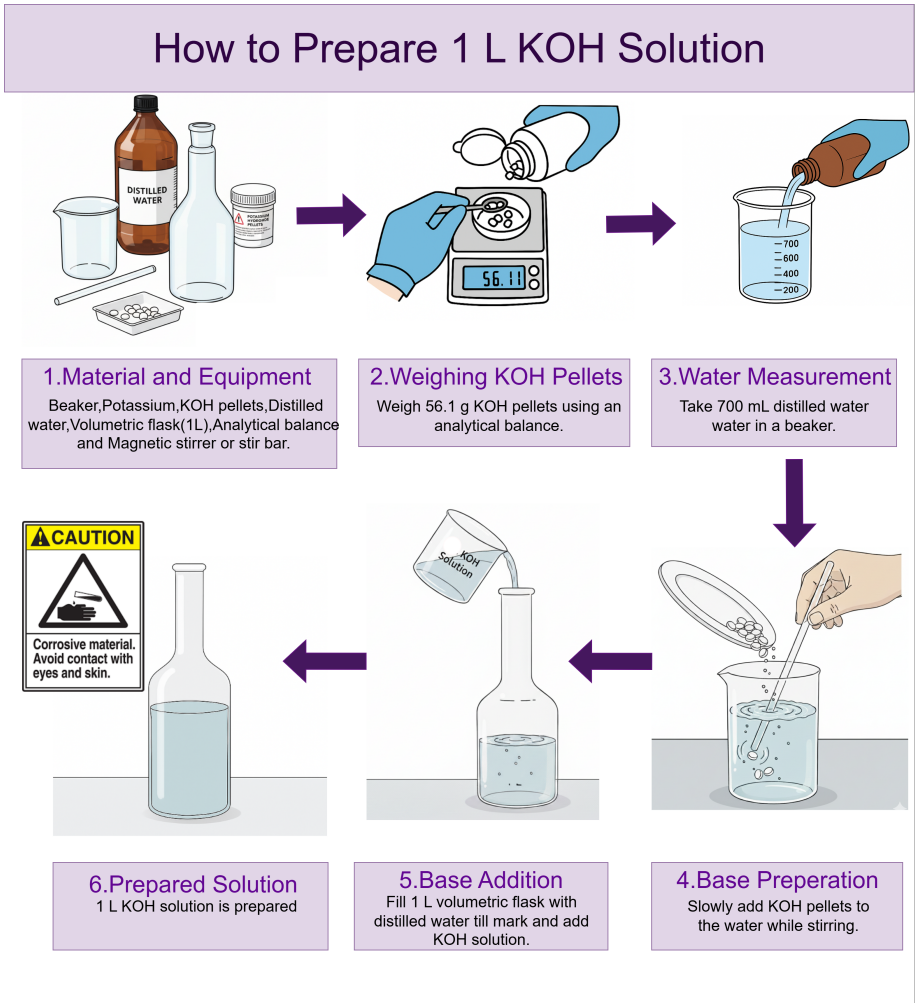

Figure 5.1: *Step by step guideline tp prepare 1 L solution of 1 M KOH.*

To extend the range of observation and to check the accuracy of the measurements, a solution of potassium ferricyanide (KFCN) was also used. Preparation of KFCN was the same as that of KOH, only the fact that here 0.1 M solution was prepared instead of 1 M and the quantity of solute was adjusted accordingly.

5.1.2 Operational Procedure of the Potentiostat

After preparing the electrolyte solution, it was carefully poured into a 30 mL beaker, and all electrodes were thoroughly cleaned before being immersed in the solution. The working electrode (WE), reference electrode (RE), and counter electrode (CE) were then connected to the potentiostat and securely positioned in the electrochemical cell.

Once the setup was complete, the potentiostat was powered on and the control software was launched. The appropriate COM port was selected from the software settings to establish communication with the device. The voltage range for the cyclic voltammetry experiment and the desired number of cycles were defined. After confirming that all electrode connections were secure, the experiment was initiated by clicking Start all the display options are also shown in Figure 5.2. The resulting voltammogram was displayed in real time on the software interface and recorded for further analysis.

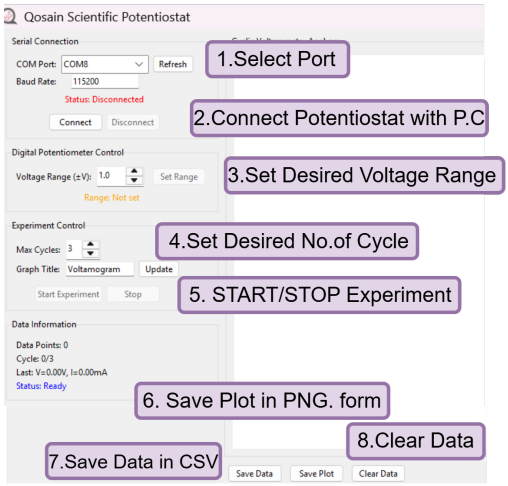

Figure 5.2: *Steps to run user-friendly potentiostat interface.*

5.2 Results

5.2.1 Calibration Testing

The two important characteristic function of any potentiostat are: the ability to precisely control the applied potential difference, and the capability to accurately measure the resulting electrochemical current [22]. To evaluate the D.I.Y potentiostat with respect to these fundamental criteria, two tests were designed under controlled conditions to characterize the operational behaviour of the device prior to its development in actual electrochemical experiment. The first test evaluated the ability of the device to generate a controlled and linear potential at the counter electrode terminal. The potentiostat output was connected across a known resistors while the DAC signal (generated through PWM filtering) was incrementally varied across the operational voltage range. The voltage response was measured using a

calibrated digital voltmeter.The measured electrode potential demonstrated a linear relationship with the programmed output values, confirming that the output driver stage maintains proportional voltage control . Any deviation from the ideal linear case was within the expected tolerance limits of the passive and active components used in the design. To further evaluate the potentiostat under dynamic operating conditions, a linear voltage scan of ± 1V at a rate of 16 mV/s was applied across a precision 1 kΩ load (±1 %). The resulting I–V curve (Figure 5.3) exhibited a strong linear correlation, demonstrating that the system maintained accurate current tracking throughout the scan. Based on the filtered slope of the current response, the calculated load resistance was 1230 Ω, in average agreement with the multimeter-verified value of 987 Ω. These tests confirms that the device can reliably

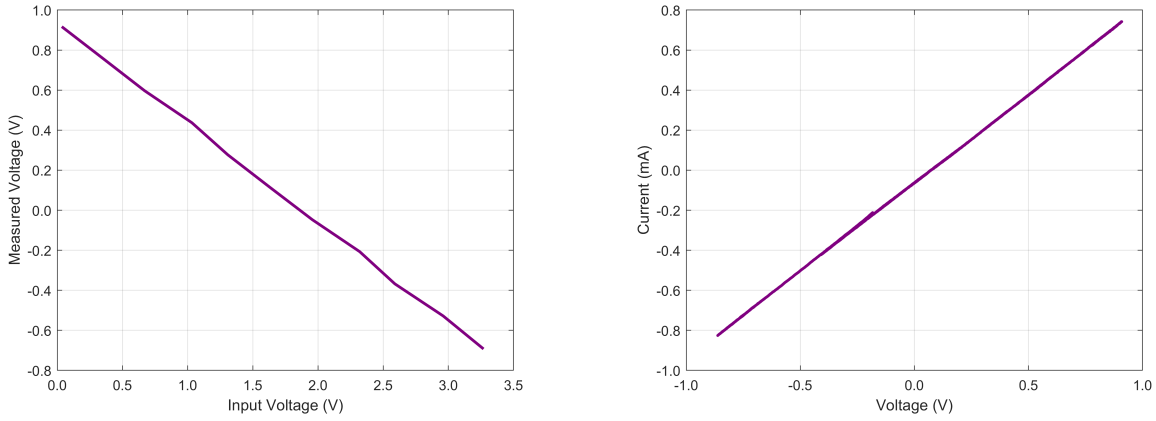

Figure 5.3: *Results of the calibrations and initial bench tests. (Left)The output of the D.I.Y potntiostat showing the ability of the device at producing a variety of output voltages. (Right)Voltammogram of the D.I.Y potentiostat when connected across a 1 kΩ resistive load. The results are within the precision rating of the resistor and are the nearly same as the measured value using a multimeter.*

perform potential sweeps and capture current variations without distortion, validating both the dynamic response of the output control stage and the accuracy of the current measurement subsystem. This method also provides a practical calibration

procedure, which may be embedded in firmware to maintain measurement accuracy during remote or long-term deployment.

5.2.2 Cyclic Voltammogram for 1 M Potassium Hydroxide

A 1 M KOH solution was used, and the potential was scanned between -1 V and $+1$ V at a scan rate of 16 mV/s. The recorded voltammograms as shown in Figure 5.4 reflect the expected behavior dominated by non-faradaic processes and water electrolysis thresholds. The results demonstrates that the D.I.Y potentiostat is capable of accurately measuring current and potential. This initial validation provides confidence in the system performance and sets a strong foundation for further characterization.

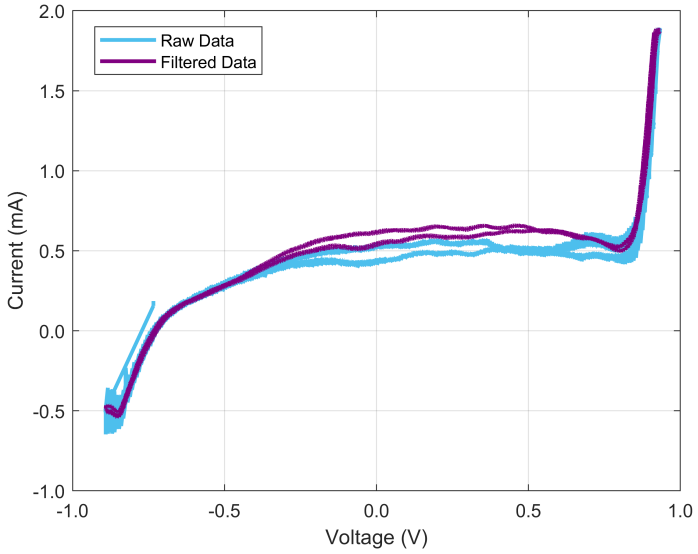

Figure 5.4: *Voltammograms of Potassium Hydro-oxide (Ag|AgCl reference electrode, carbon working electrode and gold wire counter electrode) on D.I.Y potntiostat sweeping the potential between $-1V$ and $+1V$ with raw data(blue) and filtered data(purple).*

The raw current-voltage data are depicted as blue markers, but the purple curve illustrates the same data smoothed by a Savitzky–Golay (SG) filter. The raw dataset demonstrates a high point density, it also displays baseline variations attributable to electrical noise or environmental interference. The implementation of the SG filter enhanced signal clarity, facilitating a more straightforward interpretation of the overall redox response.

5.2.3 Cyclic Voltammogram for 5mM Potassium Ferricyanide

Cyclic voltammetry (CV) was utilized to examine the redox behavior of potassium ferricyanide, a well-characterized and reversible redox system. The ferricyanide redox response forms the characteristic "duck" shape of a fully reversible reaction in the cyclic voltammogram Figure 5.5 .

During the positive (anodic) scan, the working electrode undergoes oxidation. Ferrocyanide ions, $[Fe(CN)_6]^{4-}$, lose one electron and are converted into ferricyanide ions, $[Fe(CN)_6]^{3-}$, according to the reaction at the working electrode:

$$[Fe(CN)_6]^{4-} \rightarrow [Fe(CN)_6]^{3-} + e^{-}. \tag{5.1}$$

At the same time, a complementary reduction reaction occurs at the counter electrode to maintain charge balance in the electrochemical cell:

$$[Fe(CN)_6]^{3-} + e^{-} \rightarrow [Fe(CN)_6]^{4-}. \tag{5.2}$$

During the negative (cathodic) scan, the working electrode undergoes reduction. Ferricyanide ions, $[Fe(CN)_6]^{3-}$, gain one electron and are converted back into ferrocyanide ions, $[Fe(CN)_6]^{4-}$, according to the reaction at the working electrode:

$$[Fe(CN)_6]^{3-} + e^- \rightarrow [Fe(CN)_6]^{4-} .$$

Simultaneously, the reverse oxidation reaction takes place at the counter electrode:

$$[Fe(CN)_6]^{4-} \rightarrow [Fe(CN)_6]^{3-} + e^-$$

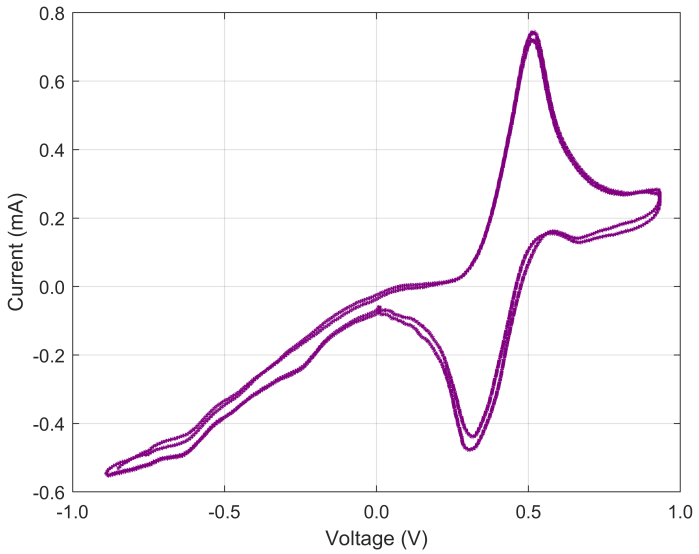

Figure 5.5: *Voltammogram of Potassium Ferricyanide (5mM solution, Ag|AgCl reference electrode, Carbon working electrode and gold wire counter electrode) on both the D.I.Y potentiostat sweeping the potential between -1 V and $+1V$.*

Overall, oxidation occurs at the working electrode during positive polarization and reduction occurs during negative polarization. The counter electrode always

supports the opposite reaction, thereby completing the electrical circuit and enabling continuous electron flow through the electrochemical system.

This combination was chosen for its stability in aquatic environments, diffusion-controlled electron transport, and distinct peak characteristics, rendering it an exemplary reference for assessing the efficacy of custom electrochemical systems.

5.3 Dynamic Range and Resolution

The dynamic range and resolution of the custom-built potentiostat are predominantly determined by the specifications of the 12-bit digital-to-analog converter (DAC) employed to produce the voltage waveform. An 12-bit DAC functioning within a ±3V range provides a voltage resolution of 4,096 discrete levels, yielding a step size of roughly 1.6 mV. This imposes quantization constraints on the potential waveform, especially in comparison to commercial potentiostats that generally provide 16-bit resolution or greater.

Notwithstanding this constraint, the system successfully generated cyclic voltammograms with adequate clarity to delineate essential electrochemical characteristics, such as oxidation and reduction peaks. Nonetheless, the diminished resolution may result in minor distortions in the curve at extremely low scan rates or when identifying small current variations near the baseline.

The scan rate is a crucial determinant affecting the precision of the response as shown in Figure 5.6. At elevated scan rates, the Arduino's constrained processor

speed and ADC sample rate may lead to timing discrepancies or delayed data gathering. The GUI implementation, along with enhanced timing control and filtering, alleviated these impacts; still, scan rates continue to constrain quick redox systems. The system offers sufficient resolution for instructional and low-to-moderate complexity electrochemical applications, while underscoring the necessity for enhancement in DAC resolution and ADC response in future iterations.

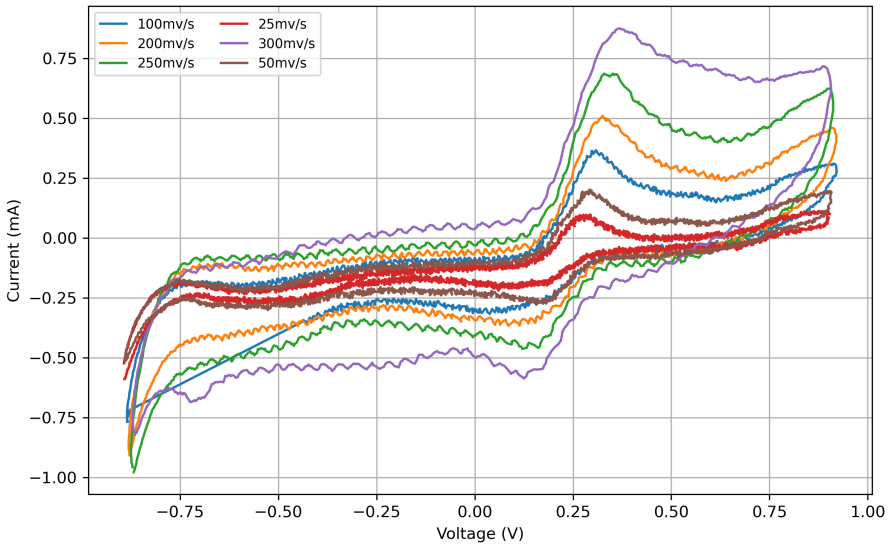

Figure 5.6: *Voltammograms of Potassium Ferricyanide on the D.I.Y potentiostat sweeping the potential between −1 V and +1 V at different scan rates. As the scan rate decreases, the voltammogram exhibits smoother and more well-defined redox peaks, indicating improved charge transfer kinetics and reduced capacitive effects. This demonstrates that lower scan rates allow the system to reach electrochemical equilibrium more effectively, resulting in clearer and more symmetric oxidation–reduction patterns.*

5.4 Cyclic Voltammetric Analysis of $K_4[Fe(CN)_6]$ at Varying Concentrations

Cyclic voltammetry was performed for different concentrations of $K_4[Fe(CN)_6$ (0.1 mM, 1 mM, 2.5 mM, and 5 mM) at scan rate of 16 mV/s to investigate the influence of the amount of electroactive species on the electrochemical response. For the lower concentrations, the cyclic voltammograms showed an almost linear shape, which indicates that the SPCE (Screen-Printed Carbon Electrode) surface behaves mainly like a capacitor rather than showing strong faradaic (redox) reactions. By increasing the concentration, the current increased throughout the whole potential window. At higher concentrations, especially at 5 mM, clear anodic and cathodic peaks started to appear, showing the expected faradaic redox activity of the ferri/ferrocyanide system. This transition from capacitive to well-defined redox peaks confirms that higher concentrations are required for both oxidation and reduction peaks to be observed clearly within the applied potential limits.

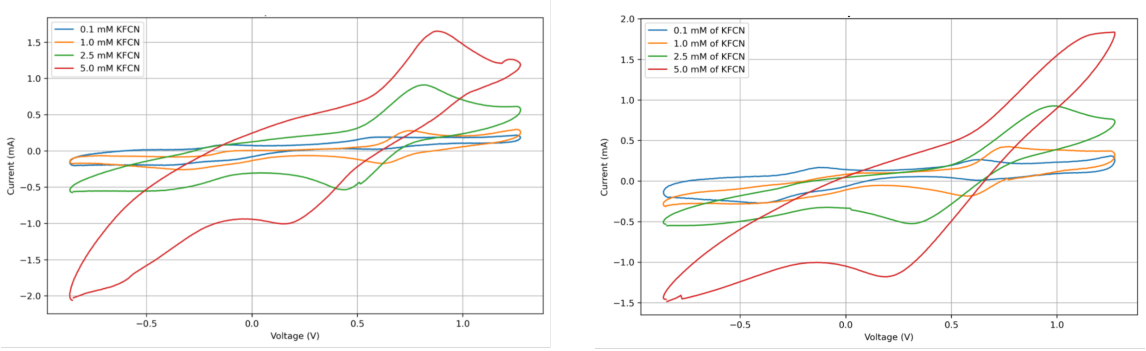

Figure 5.7: *Cyclic voltammograms of $K_4[Fe(CN)_6$ recorded at different concentrations (0.1 mM, 1 mM, 2.5 mM, and 5 mM) at (left) 16 mV/s and (right) 50 mV/s scan rates.*

To further investigate the behavior of the same concentration, CV was also performed at a higher scan rate of 50 mV/s. The results indicated that increasing the scan rate produced higher peak currents, consistent with the characteristics of diffusion-controlled electrochemical processes. Although the general peak positions were similar, the peak separation increased at the higher scan rate due to typical kinetic limitations at faster potential sweeps. The voltammograms became also more stretched and sharper in peak shape compared with those recorded at 16 mV/s. Overall, a comparison between two scan rates demonstrates that both concentration and scan rate strongly influence the cyclic voltammetric response; higher concentration improves peak visibility, while a higher scan rate increases current and affects peak symmetry and separation.

5.4.1 Scan Rate Dependence and Randles–Ševčík Analysis

After investigating the cyclic voltammetry at various scan rates for a fixed concentration of $K_4[Fe(CN)_6$ as shown in Figure 5.6. The anodic peak current, I_p, was plotted versus the square root of the scan rate ($\nu^{1/2}$), in order to verify as discussed in earlier section 3.1.4, if the redox process is controlled by diffusion according to the Randles–Ševčík equation:

$$I_p = 2.69 \times 10^5 \, n^{3/2} A D^{1/2} \, C \nu^{1/2} \tag{5.3}$$

The experimental data shown clearly reflect a linear relationship between I_p and $\nu^{1/2}$, with a slope of about 1.7975×10^{-3}, and intercept of -1.9727×10^{-4}, and a

correlation coefficient $R \approx 0.9561$. Linearity reflects that the $K_4[Fe(CN)_6$ oxidation and reduction processes at the SPCE surface are mainly controlled by diffusion and not by any surface adsorption or kinetics.

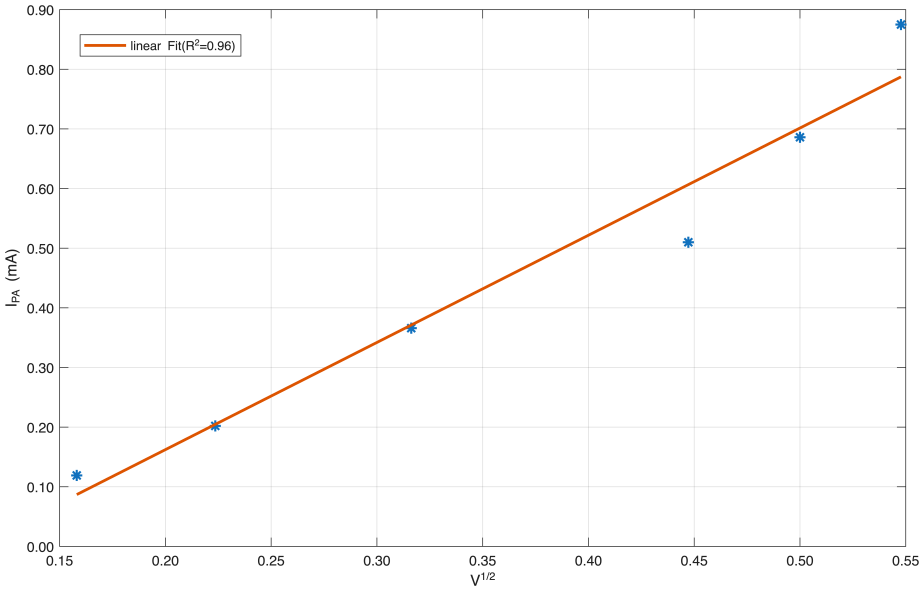

Figure 5.8: *Plot of peak current (I_p) versus square root of scan rate ($\nu^{1/2}$) illustrating the Randles–Ševčík relationship. The linear fit (slope ≈ 0.04, intercept ≈ 0.77–0.80, $R^2 \approx 0.81$) indicates a quasi-reversible electrochemical process, with the positive correlation confirming diffusion-controlled behavior of the redox species.*

The relatively high correlation coefficient reflects a strong and consistent dependence of the peak current on the scan rate, underscoring the reproducibility of the electrode response. The slope of the linear fit holds particular significance; it is directly proportional to the diffusion flux of the redox species and can be used to estimate the diffusion coefficient given the remaining parameters. In summary, this confirms the mass-transport-limited nature of the electrochemical process and constitutes a solid quantitative basis for subsequent electrochemical characterization

and modeling of $K_4[Fe(CN)_6$ at the SPCE interface.

5.4.2 Peak Currents and Diffusion-Controlled Behavior

To further investigate the redox behaviour of $K_4[Fe(CN)_6$ at 0.1, 1, 2.5, and 5 mM in 25 mL of distilled water at scan rate of 16 mV/s as already shown in Figure 5.7. Anodic peak current (I_{ap}) and cathodic peak current (I_{cp}), and their related peak potentials (Eap and Ecp) are summarized in Table 5.1

$K_4[Fe(CN)_6]$ Conc	I_{ap} (mA)	E_{ap} (V)	I_{cp} (mA)	E_{cp} (V)	$\lvert I_{cp}\rvert/\lvert I_{ap}\rvert$
0.1 mM	0.213	1.256	-0.204	-0.842	0.935
1.0 mM	0.298	1.263	-0.261	-0.328	0.872
2.5 mM	0.91	0.817	-0.575	-0.843	0.631
5.0 mM	1.652	0.879	-2.061	-0.852	1.247

Table 5.1: *Electrochemical peak data for different $K_4[Fe(CN)_6]$ concentrations.*

The experimental data in above table shows that both anodic (I_{ap}) and cathodic (I_{cp}) peak currents increase systematically with increasing $K_4[Fe(CN)_6]$ concentration, rising from 0.213 mA at 0.1 mM to 1.652 mA at 5 mM. This trend confirms that the peak currents are directly proportional to the concentration of electroactive species, and the observed pattern in our data follows the expected behavior for a diffusion-controlled redox process, as further validated by the linear relationship of I_p with the $\nu^{1/2}$ shown in Figure 5.8.

5.4.3 Peak Currents and Reversibility

The experimental data show that the anodic peak current (I_{ap}) increases with concentration, from 0.213 mA at 0.1 mM to 1.652 mA at 5 mM, indicating a higher number of electroactive species contributing to the oxidation process. The cathodic peak current (I_{cp}) also increases in magnitude but not proportionally, as reflected in the ratio I_{cp}/I_{ap} in Table 5.1. At lower concentrations (0.1 and 1 mM), this ratio is close to unity (0.935 and 0.872), suggesting near-reversible electron transfer. At higher concentrations (2.5 and 5 mM), the ratio deviates from unity (0.631 and 1.247), indicating quasi-reversible behavior, likely due to kinetic limitations or electrode surface effects.

5.4.4 Results and Nernst Equation

The formal potential, E°, represents the potential at which the concentrations of the oxidized and reduced species are effectively equal at the electrode surface. It is calculated from the anodic and cathodic peak potentials using the relation:

$$E^\circ = \frac{E_{ap} + E_{cp}}{2}$$

In the cyclic voltammetry experiments conducted, E° remains roughly constant at higher concentrations of $K_4[Fe(CN)_6]$ as in Table . This behavior is consistent with the Nernst equation (3.1.3), which indicates that the electrode potential depends primarily on the ratio of oxidized to reduced species rather than on their absolute

concentrations. At higher concentrations, although the total amount of electroactive species increases, the relative proportion of oxidized and reduced forms at the electrode surface remains essentially the same during the redox process. Consequently, the formal potential does not change significantly with concentration, demonstrating qualitative agreement with Nernstian behavior.

The peak separation, ΔE_p, defined as the difference between the anodic and cathodic peak potentials, provides insight into the reversibility of the redox reaction. It is calculated using the relation:

$$\Delta E_p = E_{ap} - E_{cp}$$

In this study, the measured ΔE_p values are significantly larger than the ideal value expected for a fully reversible one-electron system, indicating quasi-reversible behavior. This may result from kinetic limitations, such as slower electron transfer rates at the electrode surface, or from practical factors including ohmic resistance within the electrochemical cell. Despite the larger peak separation, the system demonstrates qualitative agreement with Nernstian behavior, as evidenced by the relatively constant formal potential and the expected trends in peak currents. The observation of quasi-reversibility is common in experimental systems and highlights the influence of practical electrochemical parameters on cyclic voltammetry measurements.

Overall, these results confirm that the CV measurements are reliable and that

the $K_4[Fe(CN)_6]$ redox system behaves in a manner broadly consistent with the Nernst equation, validating the accuracy of the potentiostat data under the studied conditions.

5.5 Electronic Characterization

During developement emphasis was placed on achieving high signal integrity, low noise, and stable operation while maintaining minimal power consumption. The device architecture supports accurate electrochemical analysis and can be deployed in both laboratory and portable environments. The key electrical and performance specifications of the system are summarized in Table 5.2. The electronic characteristics were measured using a Hantek DPO6104B oscilloscope and Rigol digital multimeter.

Parameter	**Specification**
Supply Voltage	±12
Output Voltage Range	±6 V
Voltage Ripple (Peak to peak)	<1%
Output Voltage Resolution	1.6 mV
Maximum Scan Rate (At Maximum resolution)	3.2 V/s
Current Measurement Range	±3 mA
Measurement Bits	12
Maximum Sampling Rate	2 kHz
Current Noise (Peak to peak)	38 μA

Table 5.2: *Performance specifications of the developed potentiostat system.*

Chapter 6

Conclusion

This research resulted in the design, development, and validation of an economical, Arduino-based D.I.Y potentiostat capable of conducting cyclic voltammetry for electrochemical investigations. The system was evaluated with a 1 mM KOH electrolyte solution and some other sample electrolytes, and the results were compared to those obtained from a commercial potentiostat. Throughout its development, the project progressed from simple command line execution in Jupyter Notebook to an enhanced graphical user interface (GUI) that facilitates real-time plotting and smoothing.

Although composed of inexpensive components, the system successfully identified critical electrochemical characteristics, including oxidation-reduction peaks and capacitive charging currents. This validated the efficacy of the hardware-software combination. Moreover, its open-source and modular architecture amplifies its educational value, providing students with insights into both electrochemistry and the

associated apparatus.

6.1 Constraints

Although the system achieved its primary goals, specific shortcomings were noted during its operation. The analogue voltage waveform was produced utilising Arduino's PWM capability and externally filtered to yield a quasi-analog signal. This approach, while cost-effective, generated ripple and quantisation noise especially noticeable at reduced scan rates or when broader voltage ranges were utilised.

The voltage and current ranges in the system are limited to ±6 V and ±3 mA . They can be readily altered by modifying the reference voltage, DAC scaling, transimpedance resistor, and power supply levels. Nevertheless, broadening the voltage range rendered the system increasingly susceptible to noise and instability, particularly in the breadboard iteration. These problems underscore the compromise between range and signal quality given limited hardware capabilities.

A further limitation is the Arduino's 12-bit analog-to-digital converter and temporal limits. At diminished current levels, the system's accuracy are compromised. Furthermore, commercial grade functionalities like as chronoamperometry, amperometry, and etc are now unsupported.

6.2 Prospective Trajectories

Future improvements to this potentiostat should concentrate on enhancing resolution, stability, and user flexibility, while maintaining a focus on cost-effectiveness.

High-resolution digital-to-analog converters (DACs) and analog-to-digital converters (ADCs) can markedly enhance performance. The incorporation of external 16-bit DACs, like the MCP4725 or DAC8562, will provide more refined and precise analog waveform production. Likewise, high-resolution ADCs such as the ADS1115 or ADS1256 would improve the accuracy of current measurements. These components are cost-effective and significantly enhance signal quality and overall system integrity.

Substituting PWM with authentic analog waveform synthesis using DACs would eradicate the ripple linked to PWM signals and enhance voltage stability. This modification is essential for creating a more pristine baseline, particularly when functioning across broader voltage ranges.

The design can be adjusted to accommodate unique voltage and current ranges, such as ±10V or greater, along with enhanced current sensitivity. The gain-setting resistors of the transimpedance amplifier can be adjusted to achieve this. To facilitate wireless functionality and autonomous data logging, components such as Bluetooth (HC-05), Wi-Fi (ESP32), or SD card modules may be integrated. These enhancements would be especially advantageous for distant or field-based investigations when direct connection to a PC is impractical.

Support for multi-channel functionality represents a potential improvement. Integrating analog switches or multiplexers would allow the potentiostat to accommodate numerous working electrodes. This functionality would enable comparative or simultaneous electrochemical analyses, enhancing the system's research utility.

6.3 Financial Analysis of Commercial Systems

The designed technology provides considerable cost benefits relative to commercial potentiostats. A standard high-performance apparatus like the Gamry Reference 600+ is priced around PKR 3–4 million (USD 10,000–15,000). Conversely, the whole Arduino-based potentiostat, which incorporates the operational amplifier (e.g., TL084 or LM324), passive components, and a fundamental PCB, was constructed at an expense of PKR 10,000–15,000.

Despite incorporating advanced features like 16-bit DACs, WLAN modules, and data logging capabilities, the overall project cost is projected to remain below PKR 8000, constituting less than 0.3% of the expense of a commercial machine. This cost-effectiveness renders the gadget optimal for classroom demonstrations, student research initiatives, and application in resource-constrained academic settings.

6.4 Concluding Observations

This effective design of a low-cost potentiostat illustrates how practical electrochemical equipment can be made accessible, modular, and instructional. The system's

capability to demonstrate redox and capacitive characteristics confirms its efficacy, and its adaptability facilitates ongoing enhancements without significant redesigns. The D.I.Y potentiostat cannot be fully replace the laboratory potentiostat but is designed to be used in situations where a full-sized lab potentiostat is impractical or impossible. Subsequent versions with improved resolution and range can increase its functionalities while maintaining cost-effectiveness. This study serves as a basis for scalable electrochemical instruments for education, research, and innovation in cost-effective environments.

Bibliography

[1] Solubility of Things. Introduction to Electrochemistry. https://www.solubilityofthings.com/introduction-electrochemistry

[2] Potentiostat. In *ScienceDirect Topics, Engineering*, Elsevier. https://www.sciencedirect.com/topics/engineering/potentiostat

[3] vonZuben,T.W.; Salles,A.G.; Bonacin,J.A. Low-cost open-source potentiostats: A comprehensive review of DIY solutions and fundamental concepts of electronics and its integration with electrochemistry. In *ElectrochimicaActa*, **498** (2024), 144619. https://www.sciencedirect.com/science/article/pii/S0013468624008594

[4] Meloni, G.N. Building a Microcontroller Based Potentiostat: A Inexpensive and Versatile Platform for Teaching. *J. Chem. Educ.* **2016**, *93* (7), 1320–1322.

[5] Gamry Instruments. Cyclic Voltammetry. https://www.gamry.com/electrochemistry-applications/cv-cyclic-voltammetry/

[6] Martínez,M.G.;etal. Monitoring, Analysis, and Quantification of Hydrogen from …; *[Journal Title]*, 2023. https://www.sciencedirect.com/science/article/pii/S0360319923010844

[7] Aikens, D.A. "Electrochemical methods, fundamentals and applications." In *Journal of Chemical Education*, 1983. https://doi.org/10.1021/ed060pA25.1

[8] Valero Vidal, C.; Igual Muñoz, A. Influence of Protein Adsorption on Corrosion of Biomedical Alloys. In *Bio-Tribocorrosion in Biomaterials and Medical Implants*; Woodhead Publishing Series in Biomaterials; Elsevier: Amsterdam, 2013; pp 187–219. https://www.sciencedirect.com/science/article/abs/pii/B9780857095404500090

[9] Amperometry. In *ScienceDirect Topics, Chemistry*, Elsevier. https://www.sciencedirect.com/topics/chemistry/amperometry

[10] Peroff, A. Chronoamperometry (CA). Pine Research Instrumentation, September 24, 2024. https://pineresearch.com/support-article/chronoamperometry-ca/

[11] Peroff, A. Chronopotentiometry (CP). Pine Research Instrumentation, September 26, 2024. https://pineresearch.com/support-article/chronopotentiometry-cp/

[12] Lazanas, A.C.; Prodromidis, M.I. Electrochemical Impedance Spectroscopy — A Tutorial. *ACS Meas. Sci. Au* **2023**, *3* (3), 162–193. https://doi.org/10.1021/acsmeasuresciau.2c00070

[13] Gamry Instruments. "Potentiostats and galvanostats." *Gamry Instruments Official Website*, 2025. https://www.gamry.com/potentiostats/browse-all-potentiostats/

[14] CH Instruments, Inc. "Electrochemical instruments." *CH Instruments Official Website*, 2025. https://www.chinstruments.com/

[15] Ossila Ltd. "Potentiostats and electrochemical instrumentation." *Ossila Official Website*, 2025. https://www.ossila.com/

[16] Metrohm AG. "Electrochemical analysis and Autolab systems." *Metrohm Official Website*, 2025. https://www.metrohm.com/en_ae.html

[17] Rowe, A.A.; Bonham, A.J.; White, R.J.; Zimmer, M.P.; Yadgar, R.J.; Hobza, T.M.; Honea, J.W.; Ben-Yaacov, I.; Plaxco, K.W. CheapStat: An Open-Source, "Do-It-Yourself" Potentiostat for Analytical and Educational Applications. *PLoS One* **2011**, *6* (9), e23783. https://doi.org/10.1371/journal.pone.0023783

[18] ChemTalk. Nernst Equation. *ChemTalk*. 2025. Available online: https://chemistrytalk.org/nernst-equation/ (accessed on December 10, 2025).

[19] Dryden, M.D.M.; Wheeler, A.R. DStat: A Versatile, Open-Source Potentiostat for Electroanalysis and Integration. *PLoS One* **2015**, *10* (10), e0140349. https://doi.org/10.1371/journal.pone.0140349

[20] A. C. Fisher, *Electrode Dynamics*, Oxford Chemistry Primers, Oxford University Press, Oxford, 1996.

[21] Elgrishi, N.; Rountree, K. J.; McCarthy, B. D.; Rountree, E. S.; Eisenhart, T. T.; Dempsey, J. L. A Practical Beginner's Guide to Cyclic Voltammetry. *Journal of Chemical Education* **2018**, 95 (2), 197–206. https://doi.org/10.1021/acs.jchemed.7b00361. *Introduces cyclic voltammetry with step-by-step guidance for new practitioners.*

[22] Adams, S.D.; Doeven, E.H.; Quayle, K.; Kouzani, A.Z. MiniStat: Development and Evaluation of a Mini-Potentiostat for Electrochemical Measurements. *IEEE Access*, **7** (2019), 31903–31912. https://doi.org/10.1109/ACCESS.2019.2902575

[23] Ainla, A.; Mousavi, M.P.S.; Tsaloglou, M.-N.; Redston, J.; Bell, J.G.; Fernández-Abedul, M.T.; Whitesides, G.M. Open-Source Potentiostat for Wireless Electrochemical Detection with Smartphones. *Anal. Chem.* **2018**, *90* (10), 6240–6246. https://doi.org/10.1021/acs.analchem.8b00850

[24] Bjerke, O. Development of a Low-Cost Potentiostat with Cyclic Voltammetry and Amperometry Techniques Implemented: A Prototype Platform for Medical Applications, M.Sc. Thesis, University of Oslo, 2020. Available at: https://community.infineon.com/.../Olav-Bjerke---masteroppgave.pdf

[25] Pine Research Instrumentation. What Is a Potentiostat and How Does It Work? https://pineresearch.com/support-article/what-is-a-potentiostat-and-how-does-it-work/

[26] MTX Labs Global. Cyclic Voltammetry. https://mtxlabsglobal.com/

cyclic-voltammetry/

[27] Horowitz, P.; Hill, W. *The Art of Electronics*, 3rd ed.; Cambridge University Press: Cambridge, 2015. *Used to explain op-amp design, gain stages, filtering, and analog circuit theory.*

[28] Arduino Team. Arduino Uno Rev3 Technical Specifications. [Online]. https://store.arduino.cc/products/arduino-uno-rev3 *Provides microcontroller specs used for PWM control and analog measurements.*